Risø-R Report

Risø-R-1555(EN)

ACCUWIND - Methods for Classification of Cup Anemometers

J.-Å. Dahlberg, T.F. Pedersen, Peter Busche

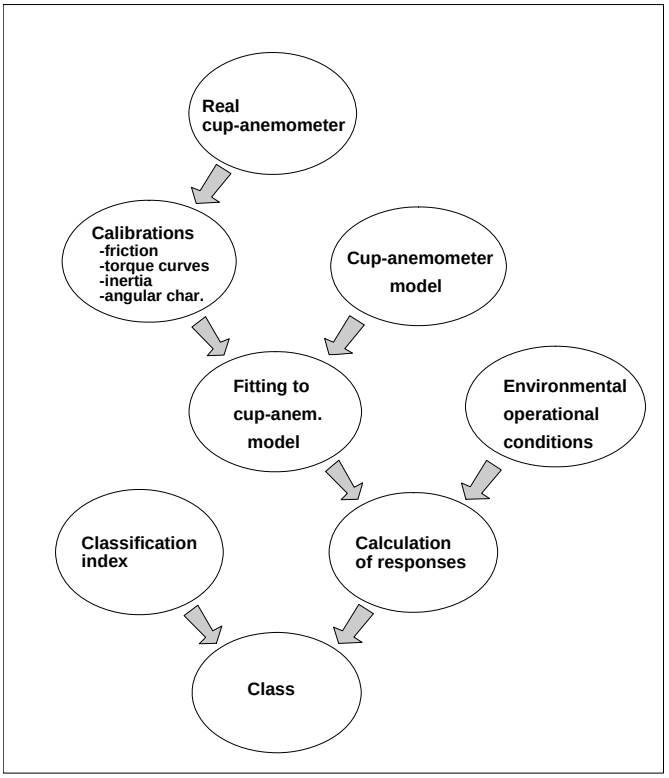

Risø National Laboratory
Roskilde
Denmark
May 2006

www.PartoSystem.com

Abstract Errors associated with the measurement of wind speed are the major sources of uncertainties in power performance testing of wind turbines. Field comparisons of well-calibrated anemometers show significant and not acceptable difference. The European CLASSCUP project posed the objectives to quantify the errors associated with the use of cup anemometers, and to develop a classification system for quantification of systematic errors of cup anemometers. This classification system has now been implemented in the IEC 61400-12-1 standard on power performance measurements in annex I and J. The classification of cup anemometers requires general external climatic operational ranges to be applied for the analysis of systematic errors. A Class A category classification is connected to reasonably flat sites, and another Class B category is connected to complex terrain, General classification indices are the result of assessment of systematic deviations. The present report focuses on methods that can be applied for assessment of such systematic deviations. A new alternative method for torque coefficient measurements at inclined flow have been developed, which have then been applied and compared to the existing methods developed in the CLASSCUP project and earlier. A number of approaches including the use of two cup anemometer models, two methods of torque coefficient measurement, two angular response measurements, and inclusion and exclusion of influence of friction have been implemented in the classification process in order to assess the robustness of methods. The results of the analysis are presented as classification indices, which are compared and discussed.

ISBN 87-550-3514-0

www.PartoSystem.com

Contents

Preface 4

1. Introduction 6

2. Classification Procedures 6

2.1 Classification Principles 6
2.2 Classification index 8
2.3 Defining Measured Wind Speed 9

3. Laboratory and Wind Tunnel Tests – Calibrations 10

3.1 Equipment 10
3.1.1Wind Tunnel LT5-II 10
3.1.2The tilt device 11
3.1.3The gust generator 11
3.1.4Light propellers to measure instantaneous wind speed 12
3.2 Conversion of pulse trains to wind speed and angular speed 12
3.3 Calibration of the tooth wheel signature 13
3.4 Normal Calibration of the Anemometer and the four propeller anemometers 14
3.5 Tilt Response Measurements 16
3.6 Static Torque Measurements at Horizontal flow and Forced Off-Equilibrium Speed Ratio 18
3.6.1Torque measurements on the classical Thies cup anemometer. 18
3.6.2Torque measurements on RISØ P2546 cup anemometer. 19
3.7 Dynamic Torque Coefficient Measurements at Horizontal Flow 22
3.7.1Gust tests with the classical Thies cup anemometer 22
3.7.2Derivation of torque characteristics 25
3.7.3Comparison of Cq derived from gust tests and torque measurements 26
3.7.4Discussion 27
3.8 Combined tilt and ramp-gust tests 28
3.9 Comparison of dynamic torque measurements with angular response measurements 29
3.10 Gust Run Measurements at Horizontal Flow 30
3.11 Step Response Measurements 32
3.12 Bearing Friction Measurements 34
3.13 Rotor Inertia Measurements 39

4. Time Domain Modelling of Cup-Anemometers 40

4.1 Introduction 40
4.2 Generalization of the rotor torque 40
4.3 The Tilt-Response & Torque-Coefficient Model (TRTC) 42
4.4 The Inclined-Flow-Torque-Coefficient Model (IFTC) 45

5. External Conditions for Cup Anemometer Classification 46

5.1 External Operational Conditions 46
5.2 Wind speed range 47
5.3 Turbulence ranges 47
5.3.1Turbulence intensity levels 47
5.3.2Turbulence spectra 48
5.4 Air temperature ranges 50

www.PartoSystem.com

5.5 Air density range 50
5.6 Flow inclination angle ranges 50
5.7 Artificial 3D Wind Generators 51

6. Application of Classification Procedures 52

6.1 Classification of cup anemometers 52
6.2 Robustness of applied procedures 52
6.3 Calibration Robustness 52
6.3.1 Differences in normal calibrations 52
6.3.2 Differences in tilt response measurements 53
6.3.3 Differences due to inertia 55
6.4 Cup Anemometer Model Robustness 56
6.4.1 Simulation of normal calibration 56
6.4.2 Comparison of measured and calculated step response 57
6.4.3 Comparison of measured and calculated response from gust runs 57
6.5 Robustness of Classification 58
6.6 Free Field Comparison Tests 61
6.6.1 Free Field Tests Compared to Simulations 61
6.6.2 Influence of Free Field Horizontal Shear Flow 62

7. Conclusions 63

8. References 66

www.PartoSystem.com

Preface

This report presents results of a European research project ACCUWIND on improvement of evaluation and classification methods of cup and sonic anemometry. The report presents results of task 1 on cup anemometry. The six ACCUWIND partners are:

- *Risø National Laboratory, RISØ, Denmark*
- *Deutsches Windenergie Institut Gmbh, DEWI, Germany*
- *Swedish Defence Research Agency, FOI, Sweden*
- *Centre for Revewable Energy Sources, CRES, Greece*
- *Energy Research Centre of the Netherlands, ECN, the Netherlands*
- *Universidad Politechnica de Madrid, UPM, Spain*

The work was made under contract with the European Commission, project number NNE5-2001-00831. Additional support to this part of the project was given by Risø (Risø National Laboratory, DK) and FOI (Swedish Defence Research Agency, SE)

www.PartoSystem.com

1. Introduction

The cup anemometer is the standard instrument used for mean wind speed measurement in wind energy. It is being applied in very high numbers around to world on masts for wind energy assessments. It is applied exclusively for accredited power performance measurements for certification and verification purposes, and for purposes of optimisation in research and development. In the area of verification manufacturers and wind farm owners sign contracts that specify clearly when a power performance evaluation is acceptable or not. The use of one type of cup anemometer might give acceptance of the performance while another one does not. The EU project SITEPARIDEN [1,2,3,4] showed measured differences between various types of cup anemometers up to 4%, which is significant when the limits of power performance acceptance is 95% of guaranteed. The EU project CLASSCUP [5,6] proved that the reason for these differences were angular response, dynamic effects and bearing friction characteristics, which differs on various types of cup anemometers.

This ACCUWIND report on cup anemometry deals with establishment of robustness in classification by focus on methods and procedures for assessment of characteristics of cup anemometers. The methods and procedures provide a platform for use in the IEC61400-12-1 standard on power performance measurements [7], as well as for development of improved instruments.

The improvement of accuracy of wind speed measurements is not an easy task. Uncertainties in each aspect of measurement, from detailed design of sensor, calibration, application on tall masts, to operational characteristics for wide ranges of climatic conditions all ads up to high uncertainties.

The problems addressed in this report are subject to a number of innovative methods. An advanced wind tunnel procedure with dynamic inflow is applied to the sensors to measure indirectly the torque characteristics without physical interference with the cup anemometer rotor, robust rotor torque measurements on cup anemometers are developed, and dynamic vertical inflow characteristics of cup anemometers are quantified.

The present report primarily focus on assessment methods for robust classification of cup anemometers, while a second report [8] presents results of the methods being applied on five different types of cup anemometers.

2. Classification Procedures

2.1 Classification Principles

Evaluation of cup anemometers must be related to the applications, under which they are applied in the field. An evaluation may be very detailed, and in practice not easy to apply, but the evaluation can be simplified and made easier to the

www.PartoSystem.com

user when a classification procedure is applied to the evaluation. A classification procedure has the purpose of categorizing the application in terms of accuracy levels for specified external operational conditions. The task for a user is then reduced to check the external operational conditions, decide on the accuracy level with the class number, and then select the cup anemometer that corresponds to the required class.

Selection of power converters is very easy due to such a classification system for electric monitoring equipment. The classification of electric power converters is based on requirements of accuracy of the instruments being lower than a certain level (classification level) for well-defined operational ranges. In specifying the power measurement equipment for a power performance test of a wind turbine, the test engineer should look at whether the claimed uncertainty classification of the measurement equipment, particularly the current and voltage transformers and the power transducer, can be retained. Given the nature of the measurands, i.e. the expected currents and voltages, the effect on the related variables should be critically analysed.

The International Electrotechnical Commission has published class indices for power monitoring and related equipment. Power transducers are covered by IEC 60688: 1992 [9], current transformers IEC 60044-1:1996 [10], and voltage transformers by IEC 60044-2:1997 [11]. In the case of a power transducer a classification of 0.1, 0.2, 0.5 or 1 indicates that the limits of intrinsic error will be within ±0.1%, ±0.2%, ±0.5% or ±1.0% where the 'fiduciary' value is the span. In the case of current and voltage transformers, similar classifications apply.

In order to provide a classification system of cup anemometers similar in principle to the classification system of electric measuring devices, the external operational conditions shall be well-defined and operational limits for the classification shall be set up. Testing of cup anemometers by applying turbulent winds with variations in all relevant external operational conditions is very difficult. An easier task is to determine the influence of various parameters of external operational conditions under idealized conditions. In the laboratory, fundamental physical characteristics can be determined. The influence of temperature on friction can be found in climate chambers. The rotor inertia can be estimated by an oscillatory vibration method. Aerodynamic characteristics can be found by wind tunnel investigations under quasi-static or dynamic conditions. All tests, obviously, must assume that these conditions are descriptive for the characteristics of the cup-anemometers under natural field conditions. Under all circumstances, the tests made under well-controlled conditions are fundamental in prescribing the physical behaviour of the cup anemometers. The behavioural characteristics in the laboratory or in the wind tunnel do not change when the cup anemometer is put into the field with turbulent wind. The only problem is, whether the turbulent wind is influencing the cup anemometer in a more complex way than can be applied under laboratory conditions.

The three most important characteristics of cup anemometers are the dynamic effects, the angular characteristics and friction in bearings. Time domain cup anemometer models that are able to handle at least these characteristics properly, can be used in a classification procedure, for instance as described in Figure 2-1 [12]. The basic elements are robust calibration procedures, and appropriate time domain cup anemometer models. An important task is then to fit calibration data to the models so that the models at least are able to simulate the calibration tests, as well as other wind tunnel tests, like step responses and

www.PartoSystem.com

dynamic measurements. When the models are tuned with the cup anemometer data, they can adequately be applied to calculate responses of realistic environmental operational conditions.

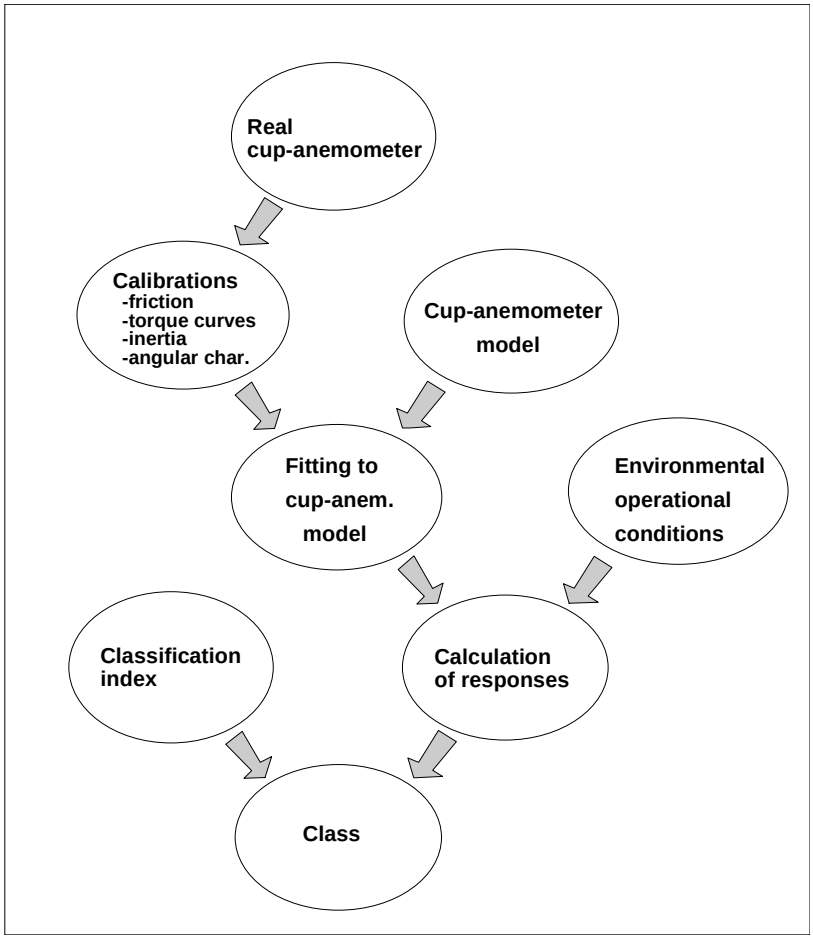

Figure 2-1 Elements of a of cup-anemometer classification from laboratory tests through time domain modelling of the cup anemometer, and calculation of responses from a modelled three dimensional wind

2.2 Classification index

The class index levels for specified external operational conditions of a classification procedure should be expressed in a way such that it is easy to derive an uncertainty estimate from a classification index number. The class index system for power converters [9] is based on systematic variations of the output signal due to variations in influence quantities, and the class index numbers are stated as integer numbers ranging over decades of levels of power. For cup anemometers the relevant class indices would not be ranging over decades, and the interesting class index numbers are within a range from zero to two or three. Therefore it is relevant to keep the class index numbers on a proportional real number scale using decimals, as proposed in the IEC standard [7]. For cup anemometers the class index numbers are not expressed as a percentage error or as an absolute error value alone because they normally have higher relative uncertainties at lower wind speeds than at high wind speeds. If percentage errors were selected for the class index number the errors at the lowest wind speeds would determine the index number. If, on the other hand, absolute errors were selected

www.PartoSystem.com

for the class index number it would be the highest winds that would dominate. In these cases it would the systematic errors in the lower wind speed range or high wind speed range, respectively, that would dominate the classification. The compromise is an index range, as stated in the IEC standard [7], which combines the absolute and the relative deviations to the class index k :

$$k = 100 \cdot \max \left| \frac{\varepsilon_i}{U_i / 2 + 5m/s} \right|$$

Where

U_i is wind speed in bin i

ε_i is the maximum systematic deviation within wind speed bin i

The systematic deviations ε_i can be derived from variations of the influence quantities: turbulence intensity, turbulence structure, air temperature, air density and average flow inclination angle. The deviations can then be plotted in a graph with the class limits as shown in Figure 2-2.

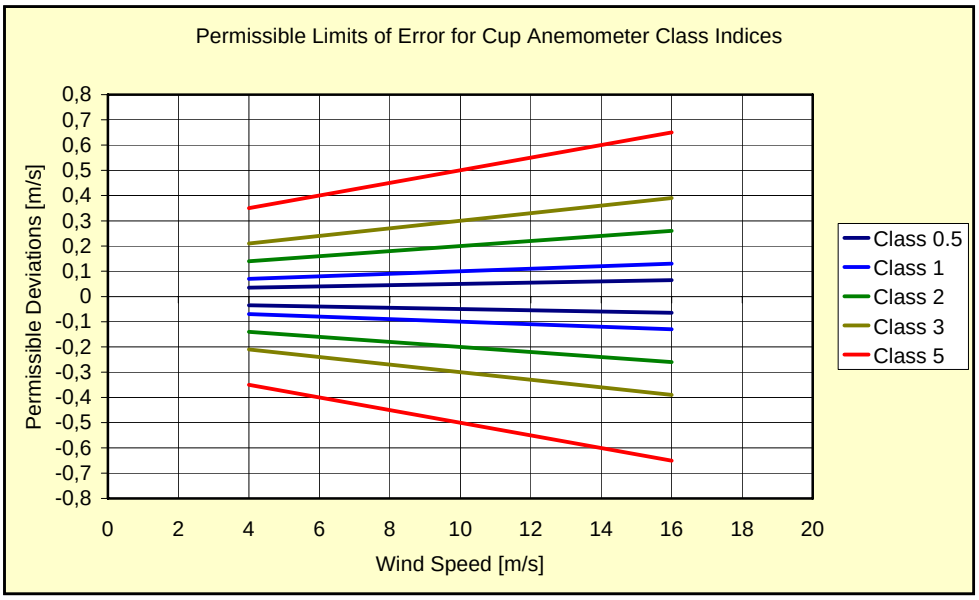

Figure 2-2, IEC61400-12-1 classification class index examples

2.3 Defining Measured Wind Speed

The measured wind speed of a cup anemometer is an averaged one-dimensional quantity. The interpretation of this quantity, though, is important in order to make a consistent classification.

Considering a time dependent 3D wind speed vector with a longitudinal component u, a transversal component v, and a vertical component w as input to the cup-anemometer.

$$\vec{U} = (u, v, w)$$

The measured wind speed of a cup anemometer, is in the IEC standard [7] defined as the “horizontal” wind speed. This definition includes only measurement of the horizontal wind speed components (length of the wind speed vector, excluding the vertical component):

www.PartoSystem.com

$$U_{hor} = \frac{1}{T}\int_t \sqrt{u^2 + v^2}\,dt$$

Or expressed as an averaged digitized measurement:

$$U_{hor} = \frac{1}{N}\sum_{i=1}^{N} \sqrt{u_i^2 + v_i^2}$$

If a cup anemometer has a cosine angular response, the vertical component w is filtered away, in which case it automatically covers the “horizontal” wind speed definition.

A vector wind speed is defined as the scalar of the “vector” of wind speed: This definition includes all wind speed components (the scalar of the wind speed vector):

$$U_{vec} = \frac{1}{T}\int_t \sqrt{u^2 + v^2 + w^2}\,dt$$

Or expressed as an averaged digitized measurement:

$$U_{vec} = \frac{1}{N}\sum_{i=1}^{N} \sqrt{u_i^2 + v_i^2 + w_i^2}$$

An analysis of the influence of the definition of the measured wind speed on power curve measurements was made in [13].

3. Laboratory and Wind Tunnel Tests – Calibrations

3.1 Equipment

3.1.1 Wind Tunnel LT5-II

All tests described in this report, except for DEWI tilt tests, referenced in chapter 6.3.2, were carried out in FOI wind tunnel LT5, which fulfils the recommendations of IEA for calibration of most used cup anemometers. The wind tunnel is shown in Figure 3-1. Tunnel data are presented in Table 3-1.

www.PartoSystem.com

Figure 3-1 The large test section of LT5. The air is sucked from right to left and is blown out through a window in the back.

Table 3-1 Wind tunnel data of FOI LT5-II (large test section)

Test section height:	0.675m
Test section width:	0.900m
Test section length:	2.5m
Test section cross section:	0.61m^2
Speed range:	~0-16 m/s
Turbulence:	< 1%

3.1.2 The tilt device

To measure the response from a cup anemometer that is exposed to non horizontal flow the pole that holds the anemometer can be tilted ±50º. The tilt tests are usually carried out such that the anemometer is slowly tilted back and force during 20 minutes. During this sequence the wind speed, tilt angle and rotational speed of the anemometer is sampled continuously. The data is processed by binning the data by tilt angle bins, and averaging the relative anemometer speed to horizontal speed.

3.1.3 The gust generator

Wind gusts can be simulated by varying the air speed of the tunnel sinusoidally. This is accomplished by means of two plates located in the outlet of the fan according to Figure 3-2.

The plates are driven by means of a three phase electric motor which is fed from a frequency converter such that the gust frequencies can be varied from 0 to 5 Hz. The plates can be driven in different ways; by keeping one plate fixed the turbulence intensity can be varied from 10 to 22 %; by rotating both plates a turbulence intensity of 32% can be reached.

www.PartoSystem.com

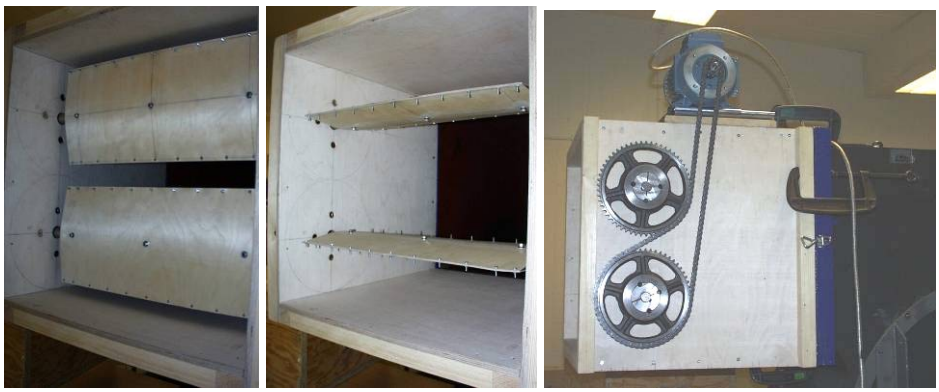

Figure 3-2 Details of the gust generator with the plates closed or opened. The plates can be driven by a chain transmission.

3.1.4 Light propellers to measure instantaneous wind speed

Special light propellers have been developed to measure rapid changes of the wind speed, see Figure 3-3. They are stream shaped from thin balsa wood and have each a weight of about 0.07 gram. The 1 mm shaft is supported by small miniature bearings. The rotational speed of each propeller is measured by equipment that consists of a laser beam and a photo sensor connected to an electronic device. The beams are directed from the outside of the tunnel through the plane of rotation of the test objects and points at the photo sensors. The rotating object (anemometer or propeller) cuts the beam and TTL pulses are creates as output.

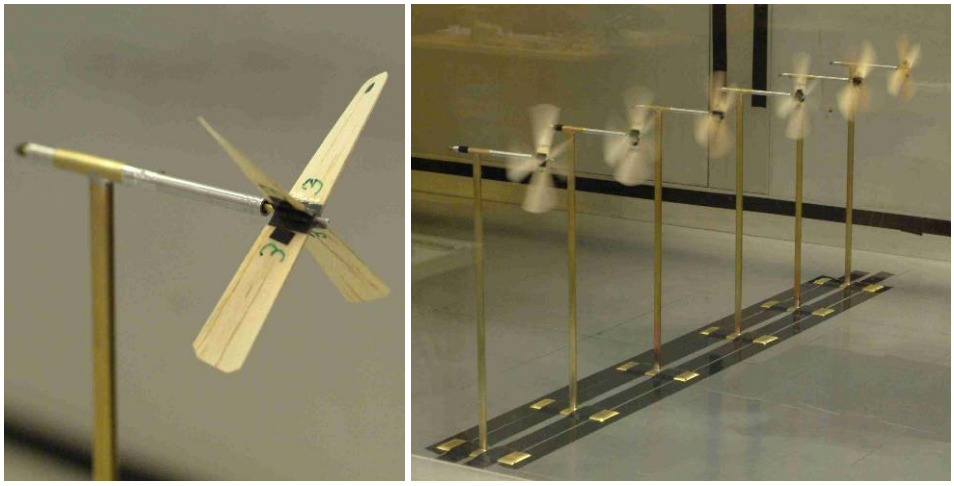

Figure 3-3 Close up view of prop 3 (left) and comparative tests to select the "best" propellers

3.2 Conversion of pulse trains to wind speed and angular speed

The conversion from pulse train frequency for the anemometer and the propellers to corresponding wind speeds are based on the calibration transfer function determined by an ordinary calibration without gusts. The instantaneous wind speed, during gust events, can be calculated from the time difference between two consecutive pulses with a time resolution given by the frequency of the

www.PartoSystem.com

pulse trains. However this method gives, due to inevitable deviations in the design of the tooth wheel, rise to significant and unacceptable scatter.

Theoretical investigations, based on an ideal anemometer, showed that it was necessary to have an, as accurate as possible, information of the rotational speed of the anemometer. This implies that it is necessary to have detailed information of the individual tooth position along the revolution. This information needs to be determined by calibration of each individual anemometer.

3.3 Calibration of the tooth wheel signature

The calibration can be carried out in two ways. Either with a fly wheel in still air or with the anemometer exposed to constant wind speed of different magnitudes as an ordinary calibration. For both methods the time between pulses are averaged and normalized.

The first method gives an absolute measure of the gap distribution (signature) of the tooth wheel and the second method gives a combined result which also includes the variations in rotational speed caused by different aerodynamic forces from the position of the cups. The latter method will give a signature that is dependent on the direction of the wind flow in relation to the fixed part, the house.

In the following Figure 3-4, Figure 3-5 and Figure 3-6, graphs are presented to demonstrate the results from calibration of the tooth wheel of the classical Thies anemometer.

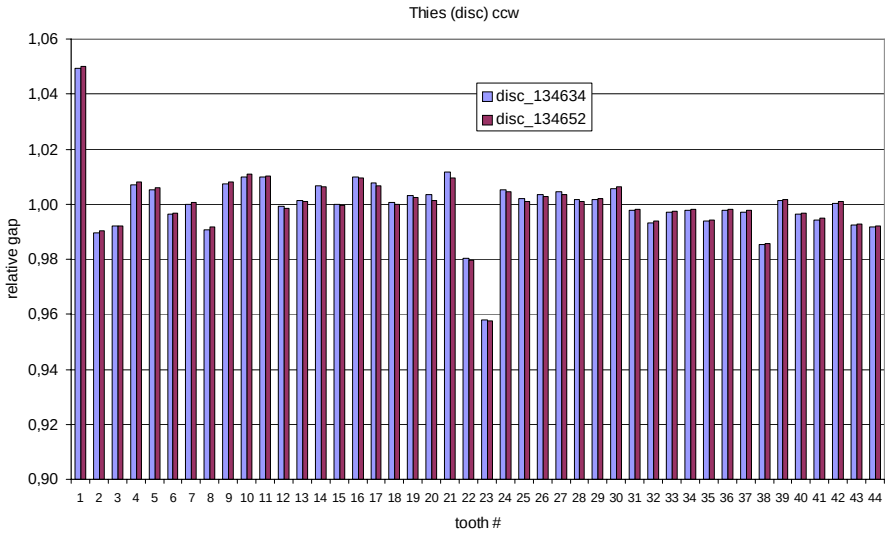

Figure 3-4 Absolute measure of the tooth wheel signature by means of disc rotation in still air. Two 10-second measurements with 100 kHz clock pulse frequency for the timing of the pulses. Note that the difference between the smallest and widest gap is about 10%.

www.PartoSystem.com

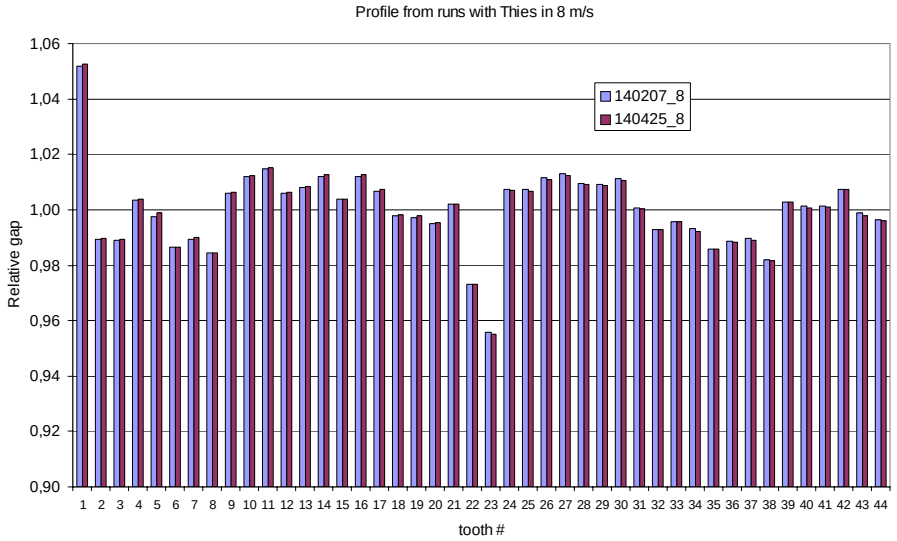

Figure 3-5 Determination of the combined tooth wheel signature derived from two 100-second measurements in 8 m/s wind speed.

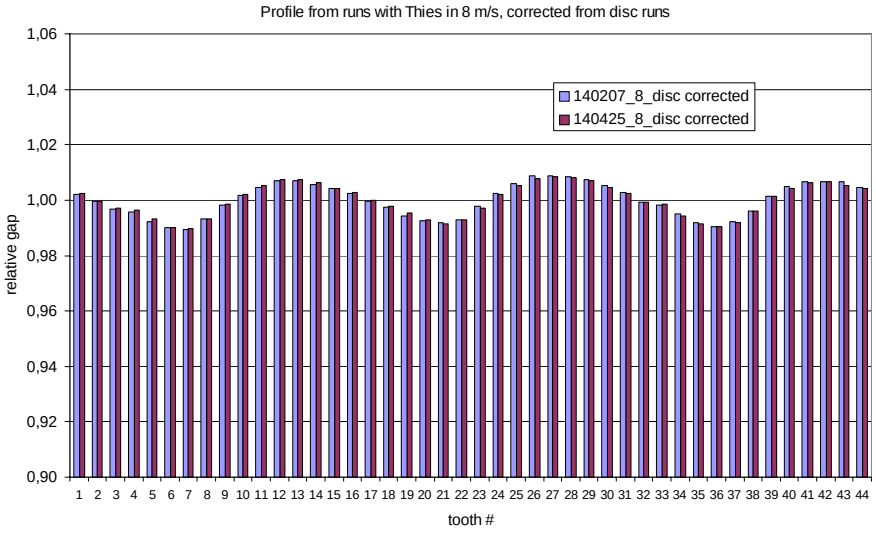

Figure 3-6 Determination of the air component in the tooth wheel signature as a result from a combination of the signatures in the figures above. The three per rev variation appears now very clearly.

3.4 Normal Calibration of the Anemometer and the four propeller anemometers

All tests are preceded by a normal calibration of the anemometer together with the four light propeller anemometers, see Figure 3-7. The propeller anemometers are used to measure the instantaneous wind speed during gust tests.

www.PartoSystem.com

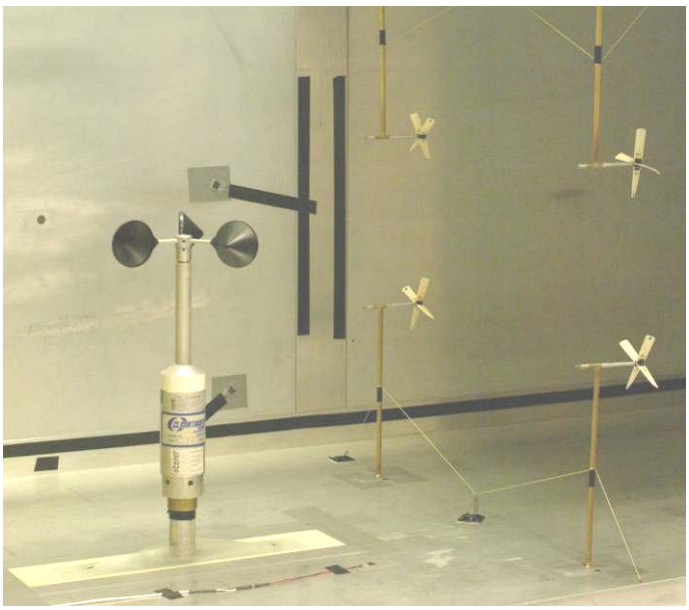

Figure 3-7 A typical setup of the anemometer and the four propeller anemometers in the LT5 wind tunnel. The wind is blowing from right to left. The upper propellers are labelled p2 and p3 from left to right and the lower propellers are labelled p4 and p5 from left to right.

The calibration procedure follows in principal an ordinary calibration. Each data point is acquired during 125 seconds. The measurement sequence starts and ends with a zero reading with the tunnel shut down. The first point is 5 m/s then 7, 9 etc. up to 15 m/s. On the way down the even wind speeds are measured.
The analogue volt values from the WT pressure transducer and tilt angle sensor are sampled at 100 Hz. The pulses from the anemometer and the propellers are clocked with a 100 kHz timer.

The evaluation procedure involves; counting of pulses, conversion of pressure signals to wind speeds and straight line fitting. A typical result is shown in Table 3-2 and Figure 3-8.

Table 3-2 Typical calibration values of the four propeller anemometers

Object	Slope	Intercept	R2	St.err.
Anem	0,0461	0,151	0,99996	0,035
P2	0,0940	-0,053	0,99999	0,017
P3	0,1036	0,195	0,99998	0,025
P4	0,1128	-0,017	1,00000	0,011
P5	0,1214	0,052	0,99994	0,040

www.PartoSystem.com

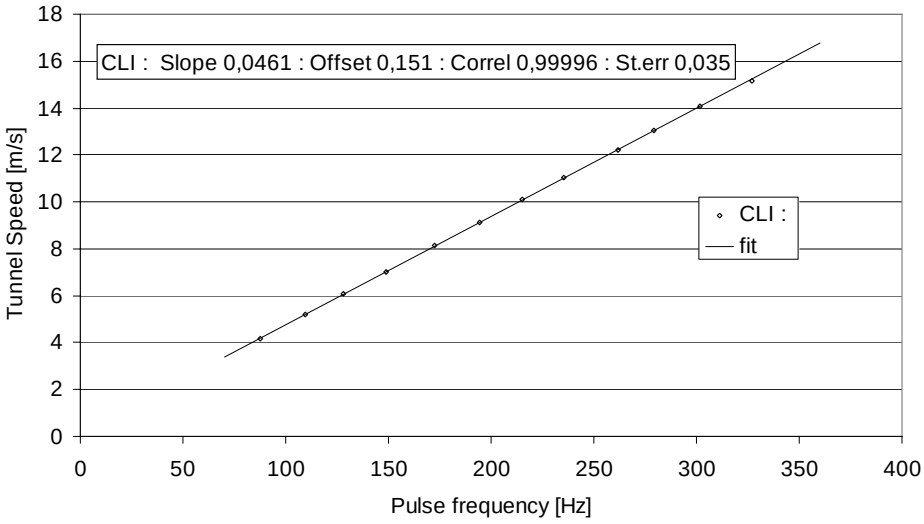

Figure 3-8 A typical result from calibration of a Climatronics anemometer over the 4-15 m/s range.

3.5 Tilt Response Measurements

During the tilt tests the anemometer is slowly (approximately 2º/sec) tilted back and forth during 1050 seconds. The tilt angle and tunnel speed are continuously measured with 20Hz and the pulses from anemometer and the four propellers are sampled with a 100 kHz clock timer. The evaluation involves conversion from pulse frequencies to wind speed by using the transfer functions from the calibration. The data are sorted into 2º tilt bins and averaged. The tilt tests are performed at wind speeds of 5, 8 and 11 m/s. Figure 3-9 shows a typical test with the cup anemometer in the extreme tilt positions. Figure 3-10 shows typical time traces of tilting angle and sensor output. Figure 3-11 shows binned results of the test, and Figure 3-12 the final angular responses of the tilt test.

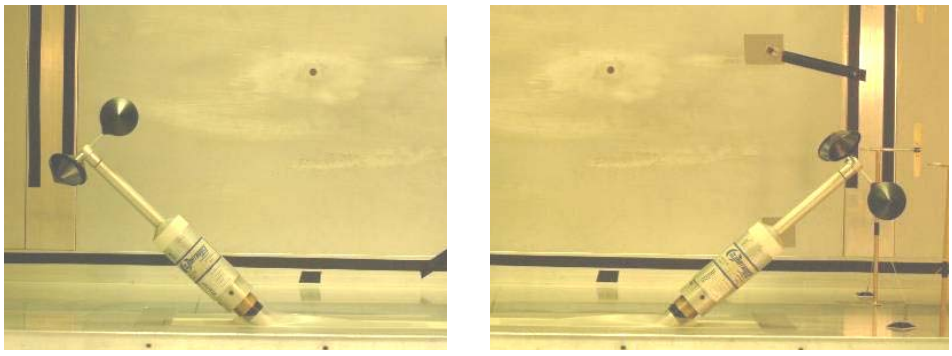

Figure 3-9 The anemometer in the -47º and +47º turning-points. Wind is blowing from right to left.

www.PartoSystem.com

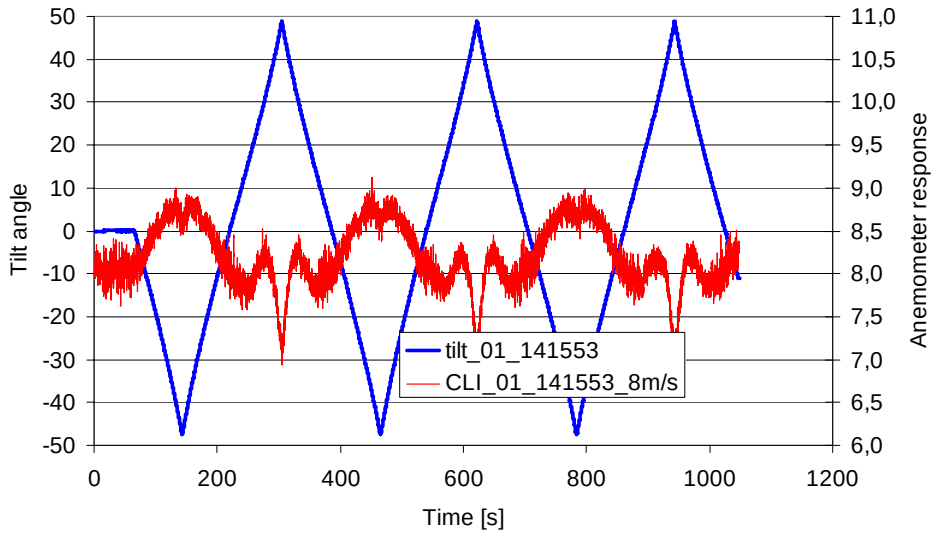

Figure 3-10 Time traces from the test with Climatronics sensor at 8 m/s wind speed. The blue curve shows the tilt angle and the red curve the anemometer response. No tilt motion is performed during the first 60 seconds to ensure that sufficient number of values fall into the zero tilt angle bin (±1°) which, during the evaluation, is used for normalisation.

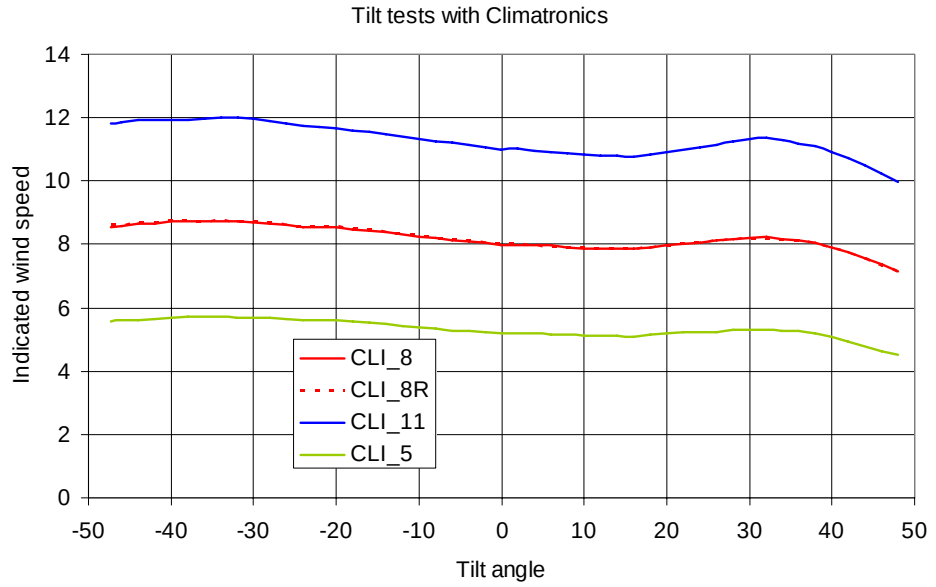

Figure 3-11 Binned results from tilt tests with Climatronics sensor at four wind speeds.

www.PartoSystem.com

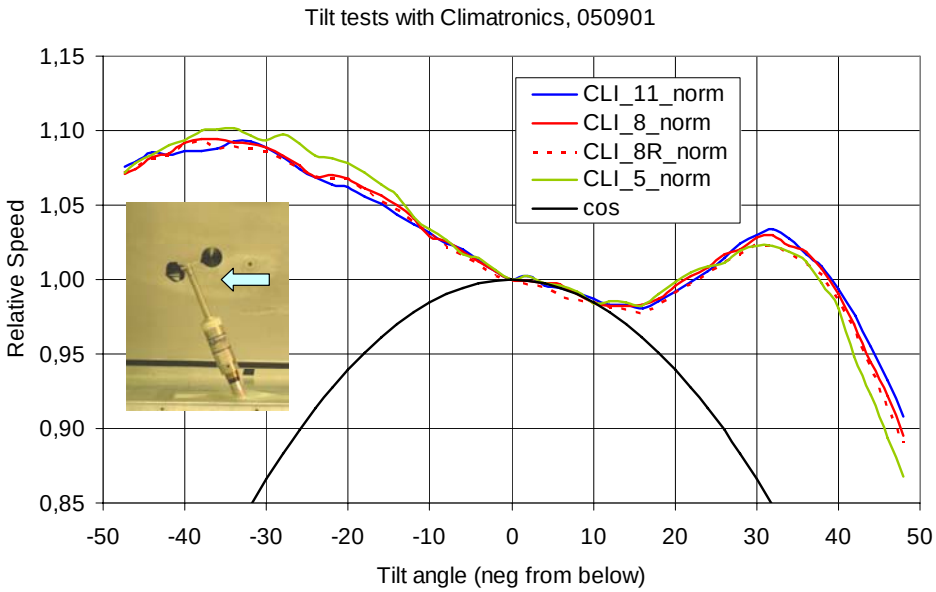

Figure 3-12 Normalised binned results from tilt tests with Climatronics sensor at all wind speeds. The values are normalised with the value in the zero bin. The anemometer significantly "over reads" the wind speeds at high negative (wind from below) inflow angles.

3.6 Static Torque Measurements at Horizontal flow and Forced Off-Equilibrium Speed Ratio

This chapter refers to a torque measurement method developed and performed prior to the ACCUWIND project [5]. The measurements refer to two cup anemometers with quite different dynamic characteristics, i.e. different torque characteristics [5,14]. The torque measurements in this chapter have not been normalized, but they can easily be normalized by the use of the normalization method described in Chapter 4.2.

3.6.1 Torque measurements on the classical Thies cup anemometer.

The torque characteristics of the classical Thies anemometer was determined by measurements carried out in the CLASSCUP project in February 2001 [5]. For those tests an external motor was driving the anemometer through a thin shaft through the wind tunnel wall, and attached to the rotor, see Figure 3-13 and Figure 3-14. The motor was attached to a linkage system such that the reaction torque could be measured.

The test was carried out such that the anemometer was exposed to constant wind speed of 8 m/s and the motor was used to drive or be driven by the anemometer and thereby force the anemometer to operate of-equilibrium.

For each setting of rotational speed all necessary parameters were acquired with 60 Hz sampling frequency during 30 seconds. The rotational speed was measured by counting pulses from the anemometer.

Figure 3-15 presents the derived torque to angular-speed relationship.

www.PartoSystem.com

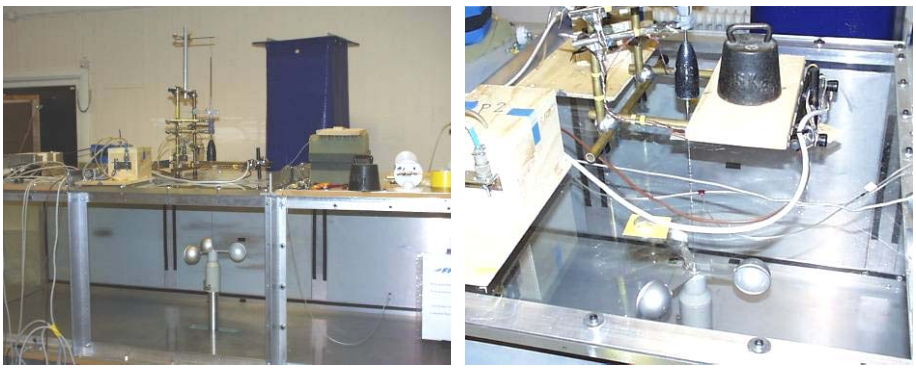

Figure 3-13 The pictures show the measurement setup for the measurement of torque from the Thies classical in LT5 2001. In the right picture the motor (black) and the thin shaft from the motor shaft to the hub of the anemometer rotor can be seen.

Figure 3-14 In the left picture the balance to measure the reaction torque can be seen.

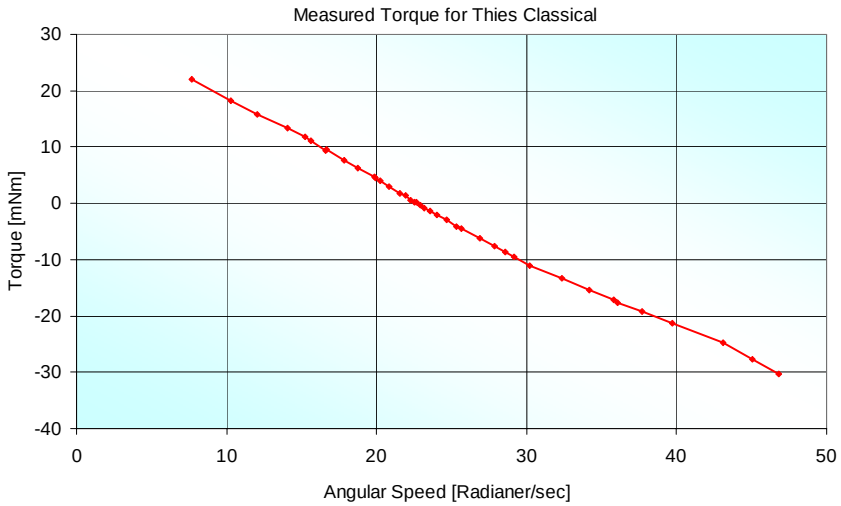

Figure 3-15 The derived torque to angular-speed relationship of Thies classical cup anemometer.

3.6.2 Torque measurements on RISØ P2546 cup anemometer.

The measurement of static torque characteristics on a RISØ P2546 cup anemometer was made at FOI in Sweden with the use of a special balance, accord-

www.PartoSystem.com

ing to [14]. A thin rod was attached to the top of the cup anemometer (seen in Figure 3-16). The rod was passed through the top of the tunnel roof (small hole in white paper) and attached to a motor (dark rotational symmetric body, see Figure 3-17). The motor was attached to a shaft that was mounted in two bearings so that the motor could rotate. The shaft was held in place by a balance, mounted on a clamp on the shaft. The balance was calibrated after the measurements.

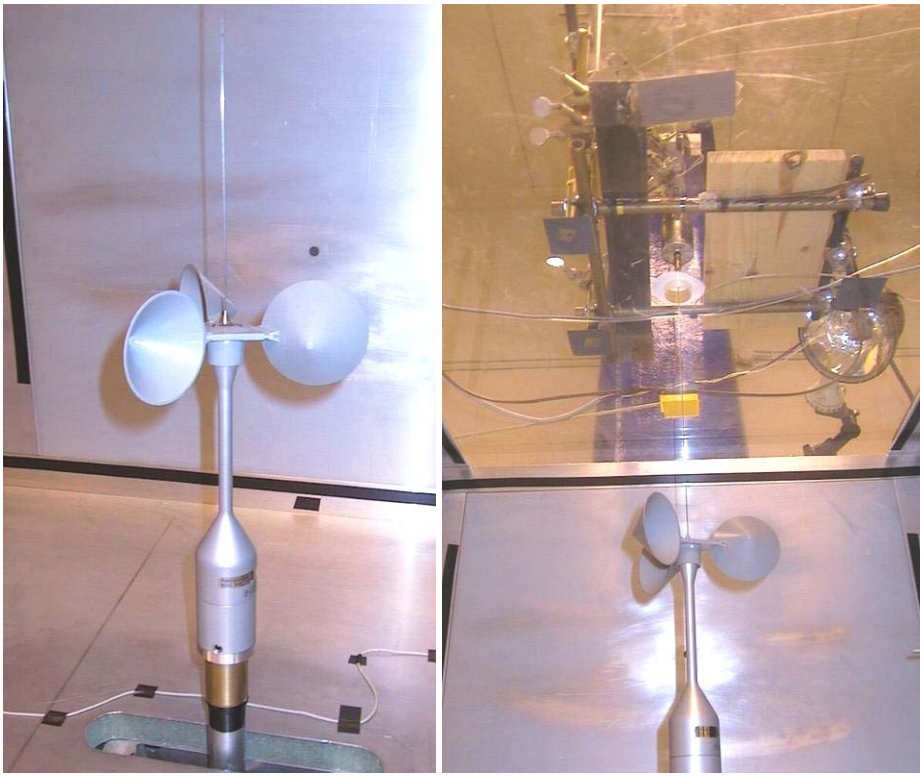

Figure 3-16 Test set-up for rotor torque measurements with thin rod mounted on top of cup anemometer and going through hole in ceiling to motor and strain gauge bridge measurement system mounted above transparent wind tunnel ceiling

www.PartoSystem.com

Figure 3-17 Torque measurement system with motor in torpedo like housing, bearings on spring loaded mounting rod in grey housing and spring balanced strain gauge bridge attached to the mounting rod to the left of the light grey attachment fixture

Torque measurements were carried out at 8 m/s at various rotational speeds, concentrated around equilibrium tip speed ratio. For each point a 30sec measurement was made. The results are shown in the following Figure 3-18.

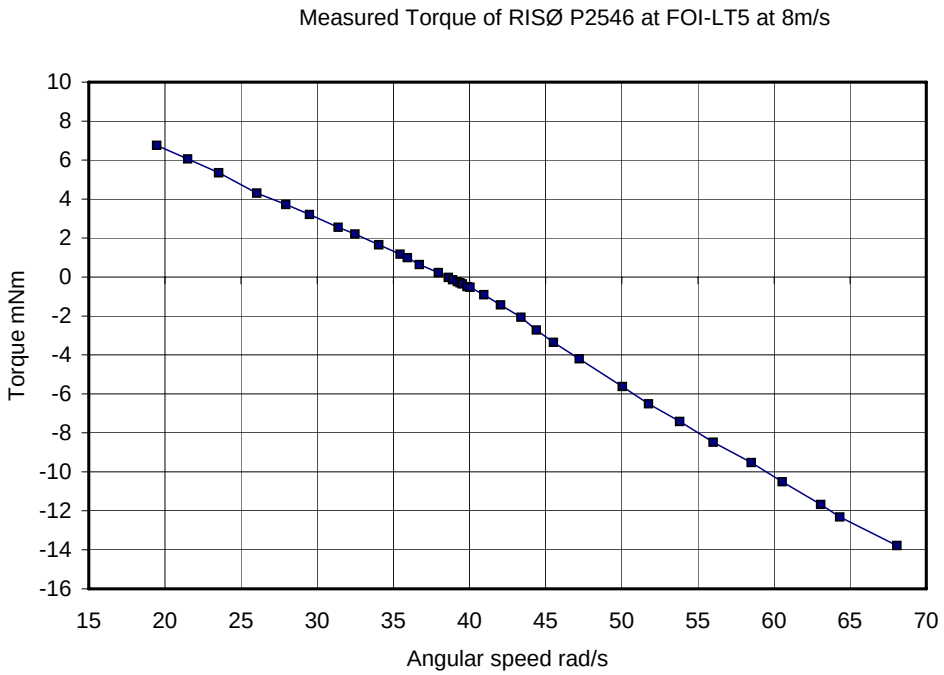

Figure 3-18 Torque measurements at FOI at 8m/s on RISØ P2546 cup anemometer [14]

www.PartoSystem.com

3.7 Dynamic Torque Coefficient Measurements at Horizontal Flow

The dynamic torque coefficient measurement method is a new method involving exposure of the anemometers to wind gusts in a wind tunnel together with accurate measurements of the instantaneous wind speed and of the rotational speed of the cup-anemometer. This method requires no attachment of a rod to the rotor as for the static torque coefficient measurement, but it requires a much higher resolution of the rotational speed. The torque-characteristics (normalised torque coefficient versus speed ratio, see Chapter 4.2) are derived indirectly from these measured time traces.

The speed sequences from the anemometer and the propellers are asynchronous in time and there is no synchronisation between the anemometer and the propellers. This is solved by linear interpolation to a common fixed time scale which is updated at a high frequency.

Once the instantaneous wind speed in the vicinity of the cup anemometer and the instantaneous angular speed of the anemometer are known, the normalised torque characteristics can indirectly be determined from the time series according to the following method.

Assuming friction to be negligible, the torque and the speed ratio are:

$$I\frac{d\omega}{dt} = Q = \frac{1}{2}\rho U^2 ARC_Q$$

$$\lambda = \frac{\omega R}{U - U_t}$$

Where:

I	rotor inertia
ω	angular speed
t	time
Q	torque
ρ	air density
U	wind speed
U_t	threshold wind speed
A	cup area
R	radius to cup centre
λ	speed ratio

From the general torque equation, a stepwise torque coefficient can be derived for small time steps, assuming constant torque over one time step.

$$C_Q \approx \frac{\Delta\omega}{\Delta t}\frac{2I}{\rho ARU^2}$$

3.7.1 Gust tests with the classical Thies cup anemometer

Tests were carried out with the classical Thies anemometer in May 2004. The tests involved ordinary calibration in the wind speed range 5-15 m/s, gust tests with various gust frequencies and one so called ramp test where the gust frequency varied linearly up and down during several minutes. Test setup is shown in Figure 3-19.

www.PartoSystem.com

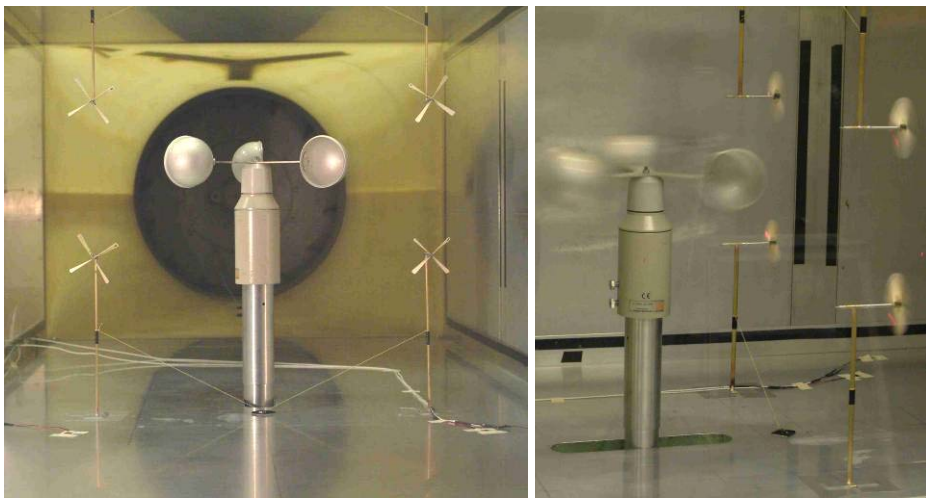

Figure 3-19 The set-up with the classical Thies cup anemometer in the centre surrounded by four propeller anemometers.

Wind sequences from air-signature corrected gust tests

The classical Thies anemometer has a tooth wheel which gives 44 pulses per revolution. The four-bladed propellers give 4 pulses per revolution. The anemometer gives typically 160 Hz and the propellers 80Hz pulse frequency at 8 m/s wind speed.

Once the tooth wheel signature derived from exposure in a constant air stream are known, all pulse measurements can be corrected such that unintentional variations in the pulse frequency caused by imperfections or cup positions can be eliminated.

In the following, results from the evaluation of the gust tests are presented. Unless otherwise stated, the following assumptions hold:

- The pulse frequencies from the anemometer were corrected with the tooth wheel signature averaged from all tests.
- The wind speed (angular speed) of the anemometer was based on the time difference between four consecutive pulses.
- The "true" wind speed, i.e. the wind tunnel speed was determined as the average of the four propeller anemometers. Their (angular speed) was based on the time difference between four consecutive pulses, i.e. complete revolutions.

Figure 3-20 shows a typical time sequence from gust tests at a constant frequency. Figure 3-21 shows a typical time sequence from a ramp gust test, and Figure 3-22 shows a smaller tooth-wheel signature corrected time sequence of the ramp gust test.

www.PartoSystem.com

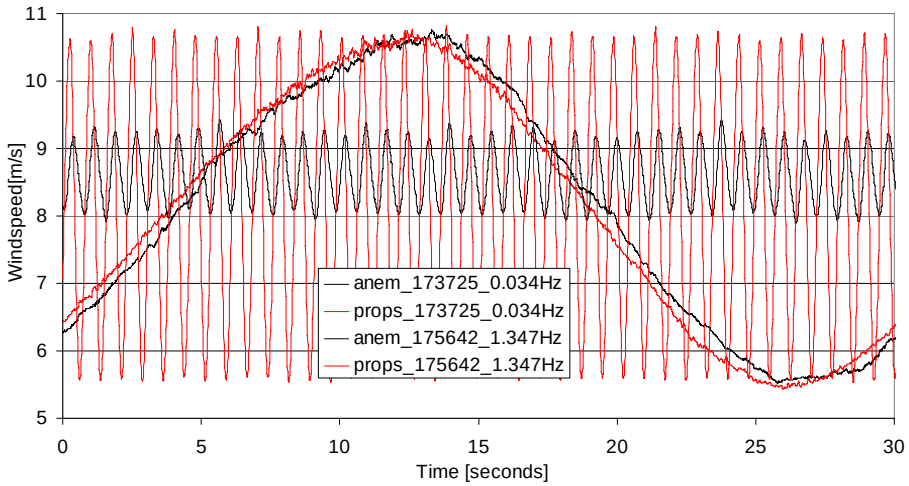

Figure 3-20 Typical time sequences from the gust tests.

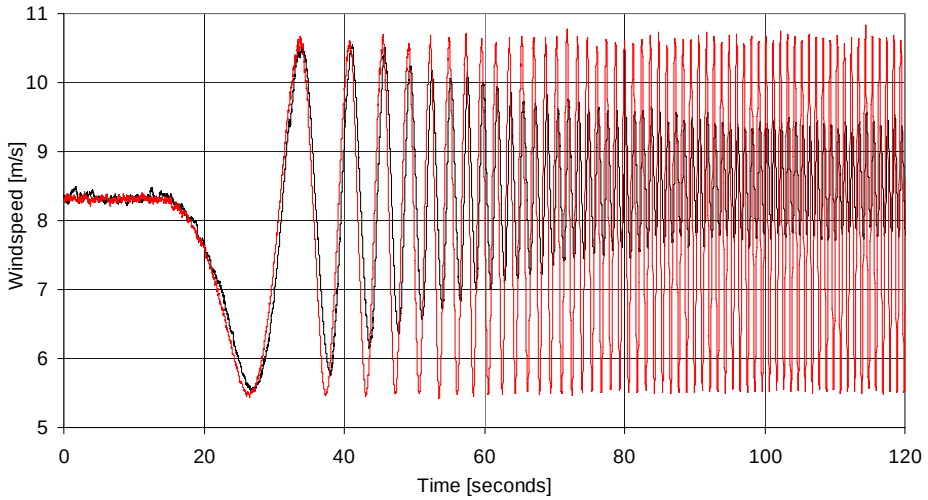

Figure 3-21 Two minutes of time sequences from the ramp gust test.

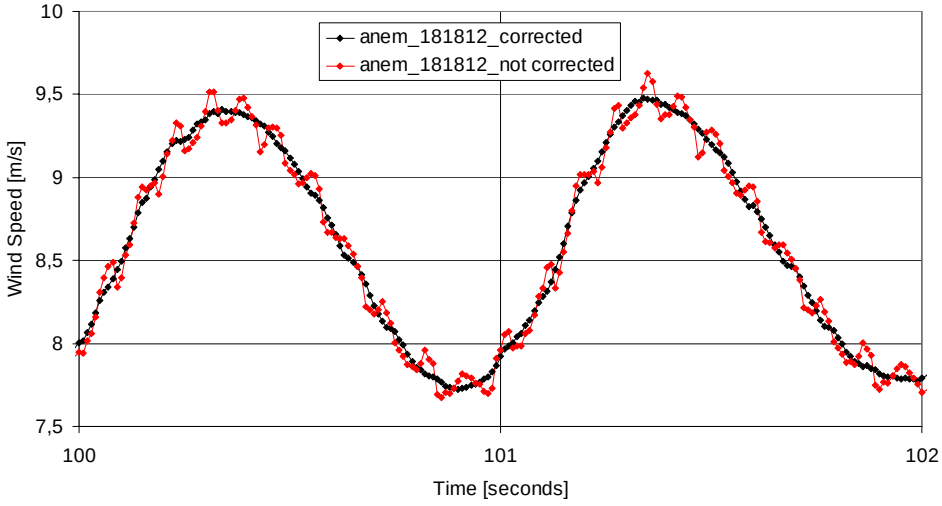

Figure 3-22 Graph of two seconds of time sequences from the previous graph with un-corrected and tooth-wheel signature corrected signals.

www.PartoSystem.com

3.7.2 Derivation of torque characteristics

The torque characteristics can now be derived from the time series according to the formula described above:

$$C_Q \approx \frac{\Delta\omega}{\Delta t}\frac{2I}{\rho A R U^2}$$

The figures from Figure 3-23 to Figure 3-26 show typical results from the evaluation.

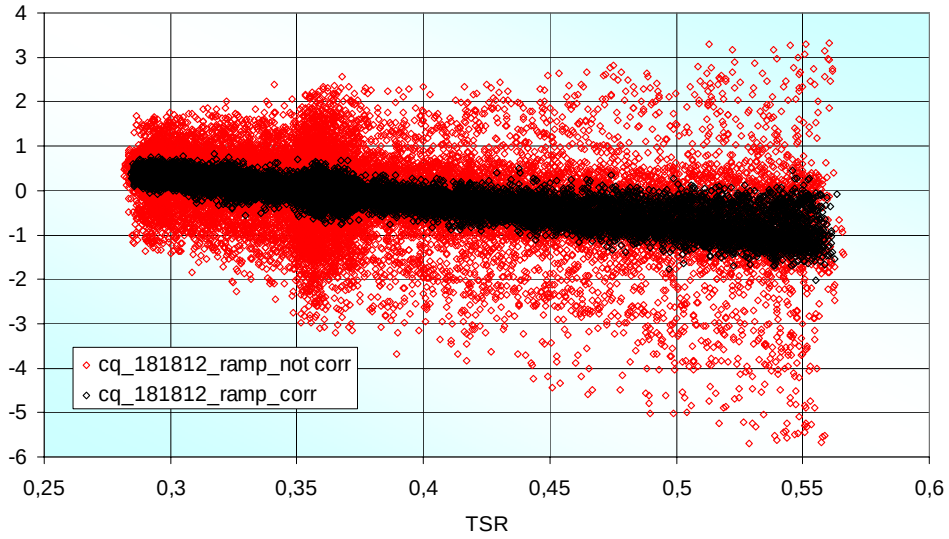

Figure 3-23 Cq derived from the corrected and the un-corrected signals. TSR is equal to speed ratio λ

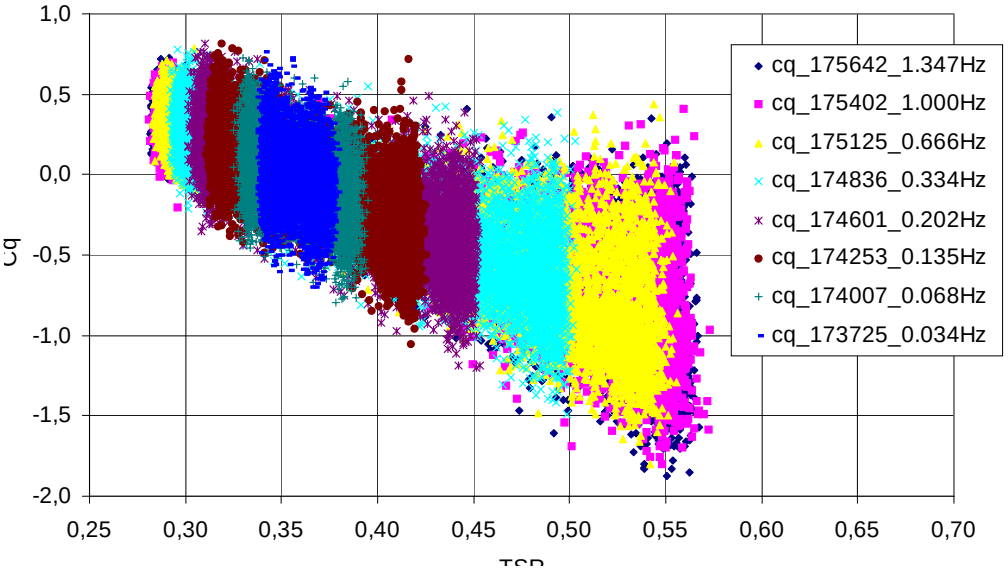

Figure 3-24 The graph presents a scatter plot of Cq derived from major parts of the gust runs. The gust frequencies are given in the legends.

www.PartoSystem.com

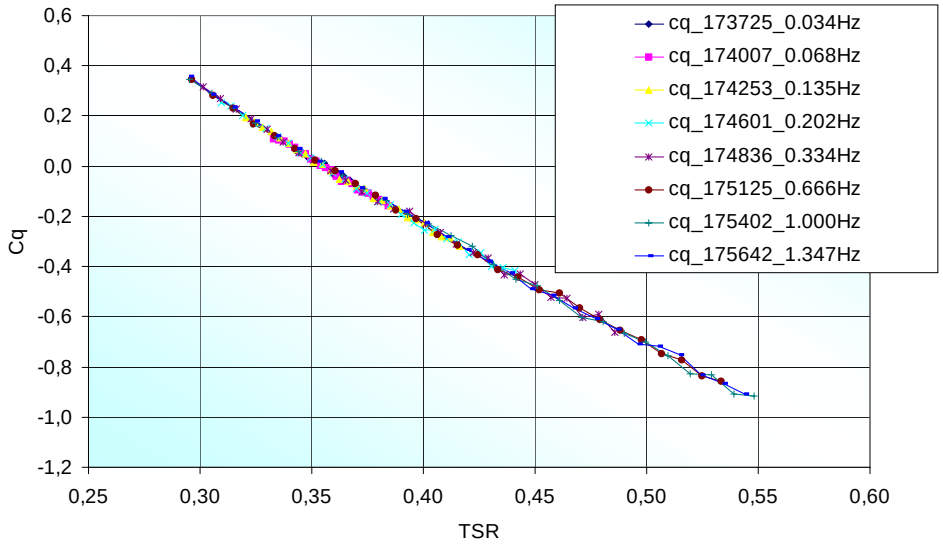

Figure 3-25 The graph presents Cq as a result of binning and averaging of the scatter from the previous graph.

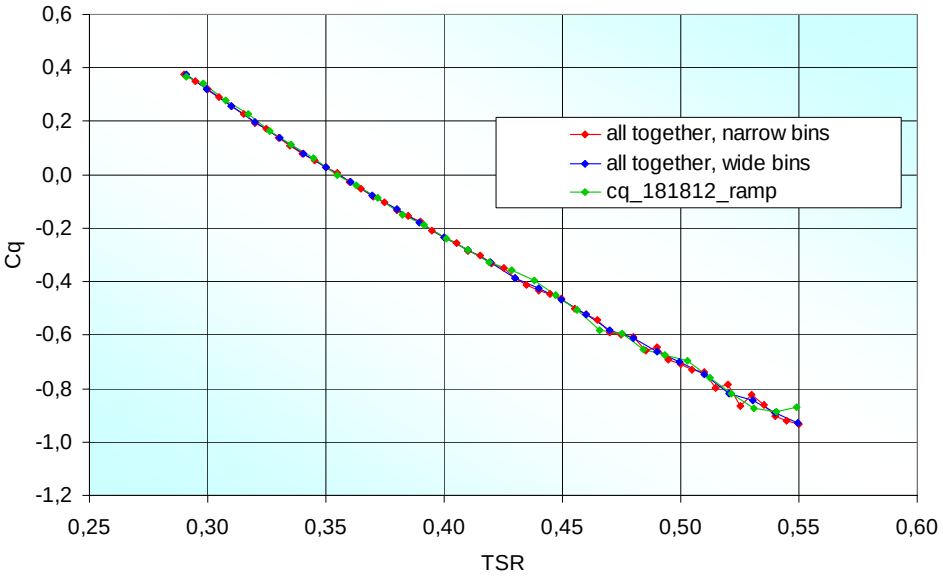

Figure 3-26 The graph presents Cq as results of binning and averaging of all data with wide and narrow bins and as the result from binning of the ramp test.

3.7.3 Comparison of Cq derived from gust tests and torque measurements

Torque curves derived by direct static torque measurements or by indirect dynamic measurements by gust runs can now be compared. A smaller correction due to variability of the wind tunnel was made.

Figure 3-27 shows a comparison of torque measurements on a Risø P2546 cup anemometer with the two different methods. Figure 3-28 shows a similar comparison for the classical Thies cup anemometer.

www.PartoSystem.com

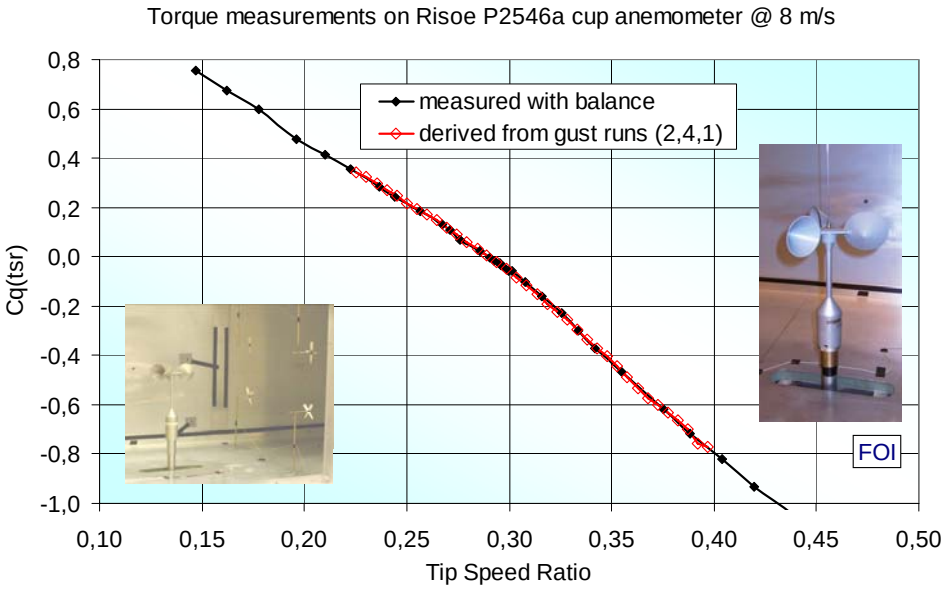

Figure 3-27 The graph shows a comparison of Cq for the Risø P2546 cup anemometer measured with the static and the dynamic torque measurement methods. Speed ratio from dynamic measurement has been offset by -0.006 and Cq scaled up by 7% (rotation around Cq=0)

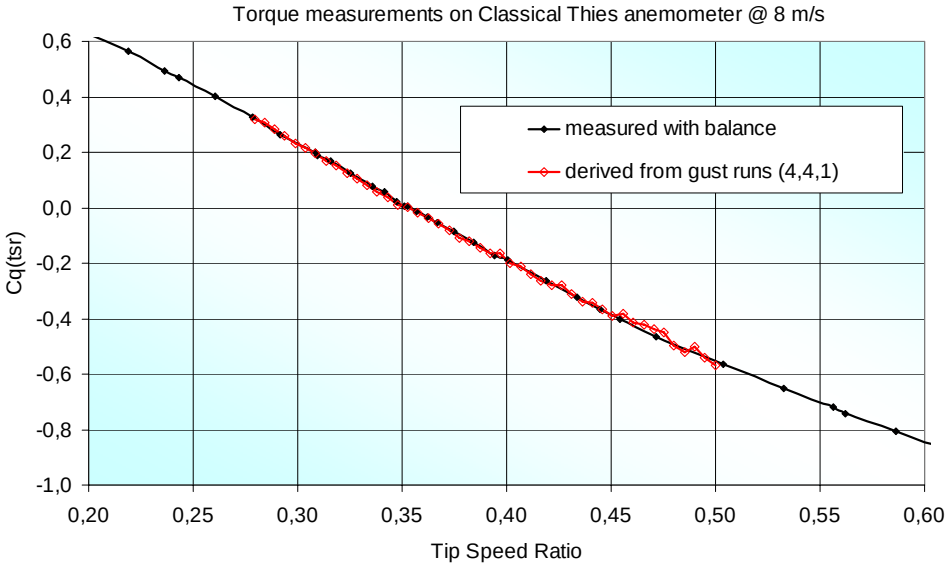

Figure 3-28 The graph shows a comparison of Cq for the classical Thies cup anemometer. Speed ratio from dynamic measurement has been offset by +0.007 and Cq scaled by 6% (rotation around Cq=0)

3.7.4 Discussion

The results presented show a good agreement between Cq derived from different test methodologies. In Figure 3-25 the comparison of Cq, based on all dynamic tests with fixed gust frequencies, show a very good agreement. Similar good agreement is found in Figure 3-26 where they are compared to the ramp gust tests.

www.PartoSystem.com

The comparisons of Cq derived from gust tests and static torque measurements, Figure 3-27 and Figure 3-28, show a very good agreement provided that the gust test results are somewhat adjusted due to variability of the wind tunnel. Tests were made at different times of the year, with different climatic conditions. Other uncertain parameters involved in the determination of Cq are the rotor inertia for the gust tests and the torque balance calibration for the static torque measurements. Adjustments carried out for the test with the Risø anemometer were a shift in speed ratio by -0.006 and a scale up of Cq by 7%. Corresponding adjustments for the Thies tests were a shift in speed ratio by +0.007 and a scale up of Cq by 6%.

The reason for the marginal speed ratio shift has not been investigated in detail but could be caused by an inherent filtering by the methods themselves. An increase in Cq value corresponds to an increase of the rotor inertia. So the need to scale up the Cq values could be caused by an imprecise determination of the inertia of the rotating parts. It can be speculated if the measurements of the rotor inertia in still air may need to be corrected with the added mass due to accompanying mass of air attached to the cup surfaces. Neither the speed ratio shift nor the Cq scale has any significant influence on the results from calculations of dynamic behaviour. A scale up of Cq corresponds to an increased torque available for acceleration of the rotation but also an increased (negative) torque available for deceleration of the rotation. It will be demonstrated later in this report that it is the details around the equilibrium, i.e. the balance between the two sides that counts.

The results of comparing the different types of torque measurements can therefore be considered very satisfactory. It is shown that it is possible to determine the torque characteristics by an indirect way, i.e. by means of gust tests. This has certain advantages, such as:

- No modification of the anemometer is necessary
- No extra components are necessary which can cause flow interference
- Test can easily be performed with inclined flow (tilting the cup anemometer)
- No balance equipment is necessary

One requirement is, of course, that access to a wind tunnel equipped with gust facilities exists and that accurate measurements of the instantaneous wind speed can be made.

3.8 Combined tilt and ramp-gust tests

In order to investigate the dynamic overspeeding for inclined flow, separate tests were carried out with combinations of inclined flow at 21 fixed tilt angles between ±47° and with gusts. The tests were carried out at 11.6 m/s tunnel speed and gust amplitudes giving approx. 32% “turbulence intensity”. The gust frequency was ramped up and down from 0-1.7-0-0.8-0 Hz during 210 seconds. Figure 3-29 shows typical time traces from the test. Figure 3-30 shows a range of torque coefficient curves derived by ramp-gust tests for the Risø cup anemometer. The torque coefficient curves can be assumed to contain essentially all necessary information that is needed on the aerodynamic forces on the cup anemometer rotor to predict the behaviour in arbitrary wind conditions.

www.PartoSystem.com

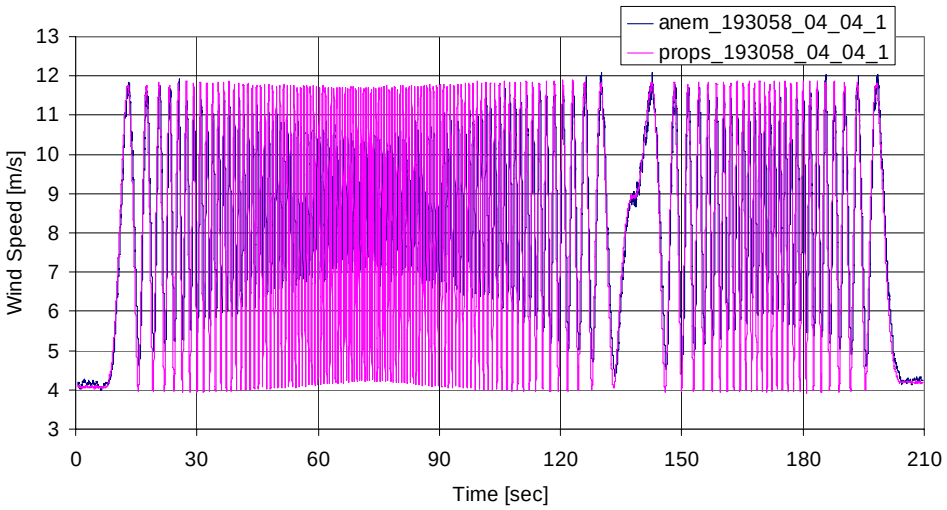

Figure 3-29 Time traces from the ramp-gust test at 0 degrees tilt angle. The graph shows the average of the four propeller signals and the cup anemometer signal from the whole 210 seconds sequence.

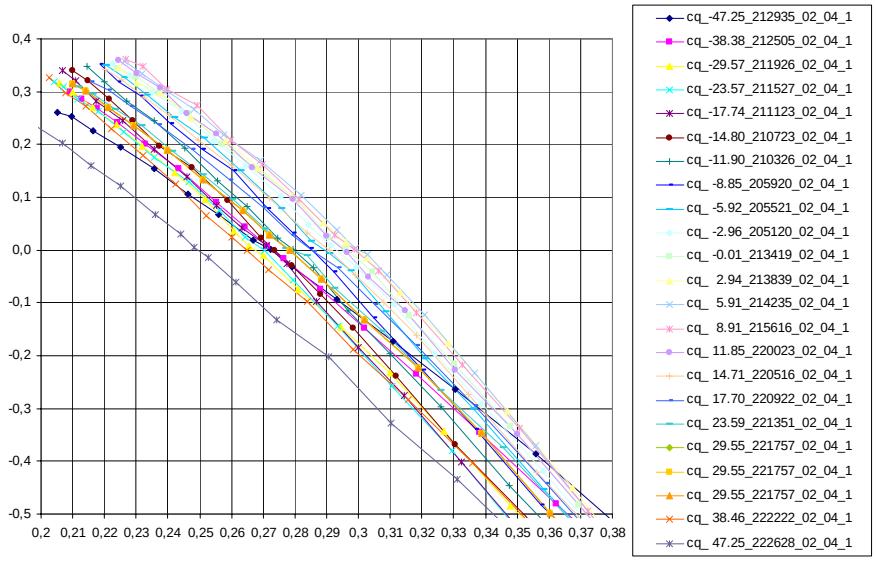

Figure 3-30 Torque coefficient curves Cq as function of speed ratio and tilt angle for the Risø cup anemometer. The curves were derived from combined tilt and ramp-gust-tests at 21 fixed inflow angles. The actual angle from each tilt setting appears in the label.

3.9 Comparison of dynamic torque measurements with angular response measurements

Obvious information, derived from the curves in the graph of Figure 3-30, are the interception points between each torque coefficient curve and the Cq=0-line. These speed ratios at various inflow angles can be normalised with the speed ratio for horizontal flow and compared with the angular response from the static tilt measurements. Figure 3-31 shows a typical comparison for a Vector cup anemometer [8].

www.PartoSystem.com

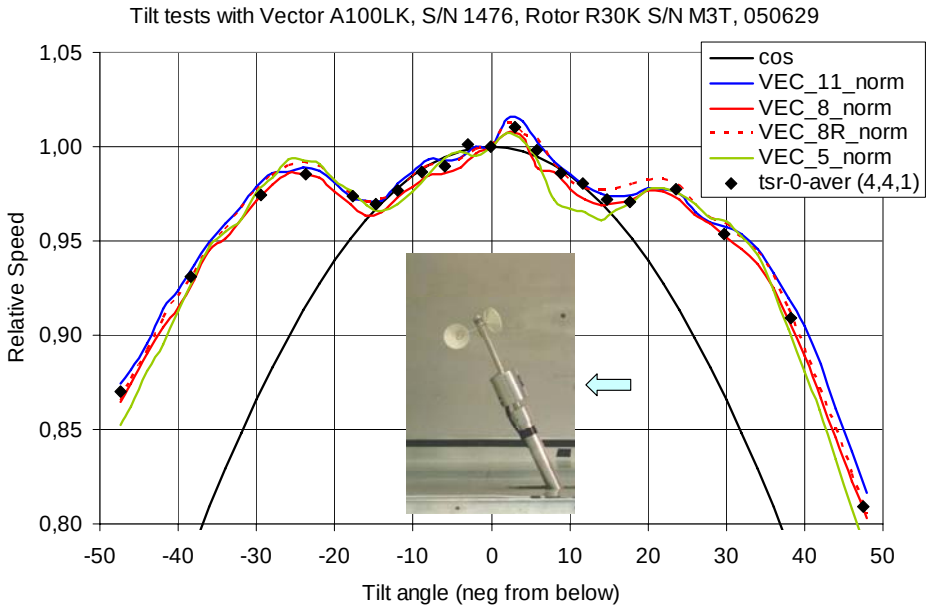

Figure 3-31 Comparison of the results from the tilt tests and the torque interception points (black diamond symbols) from the ramp-gust tests for the Vector A 100LK cup anemometer.

As can be seen from Figure 3-31 the agreement between the two types of measurements are, in this typical example, very good and convincing.

3.10 Gust Run Measurements at Horizontal Flow

Gust tests are carried out with the anemometer positioned in vertical position and exposed to sinusoidal fluctuating wind with a mean wind speed of 8 m/s and corresponding turbulence intensities of approximately 12, 16, 22 and 33%. Gust frequencies are varied from 0.018Hz (60 second cycle) up to 1.7Hz. The cup anemometer response and instantaneous wind speed from the propeller anemometers are recorded with high accuracy. This type of measurements give an indication of the tendency to overspeed under pure horizontal gust conditions, which also can be compared with the calculated response based on the measured torque coefficient curves. Gust run measurements (overspeeding measurements) are shown for a Vector cup anemometer in Figure 3-32, for a Risø cup anemometer in Figure 3-33, and for a classical Thies cup anemometer in Figure 3-34.

www.PartoSystem.com

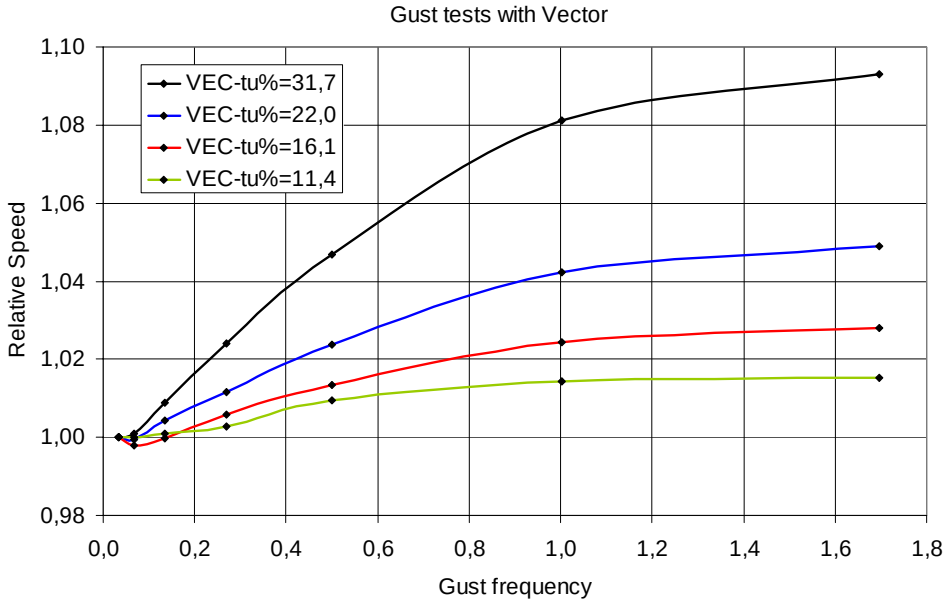

Figure 3-32 Result from gust tests with a Vector cup anemometer. The graph shows the ratio between the mean wind speed as seen by the anemometer and the average of the propellers. The highest over-speeding is about 9%.

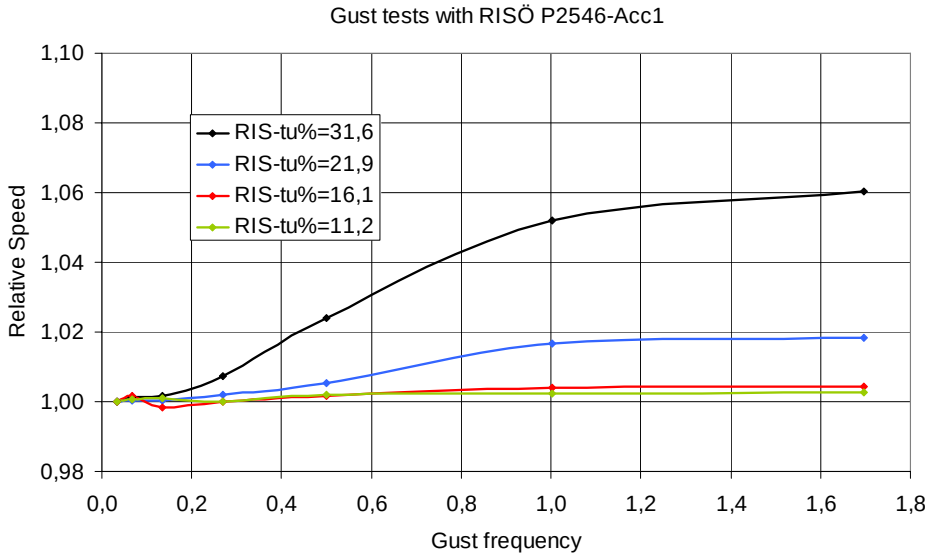

Figure 3-33 Result from gust tests with the Risø cup anemometer. The graph shows the ratio between the mean wind speed as seen by the anemometer and the average of the propellers. The highest over-speeding is about 6%.

www.PartoSystem.com

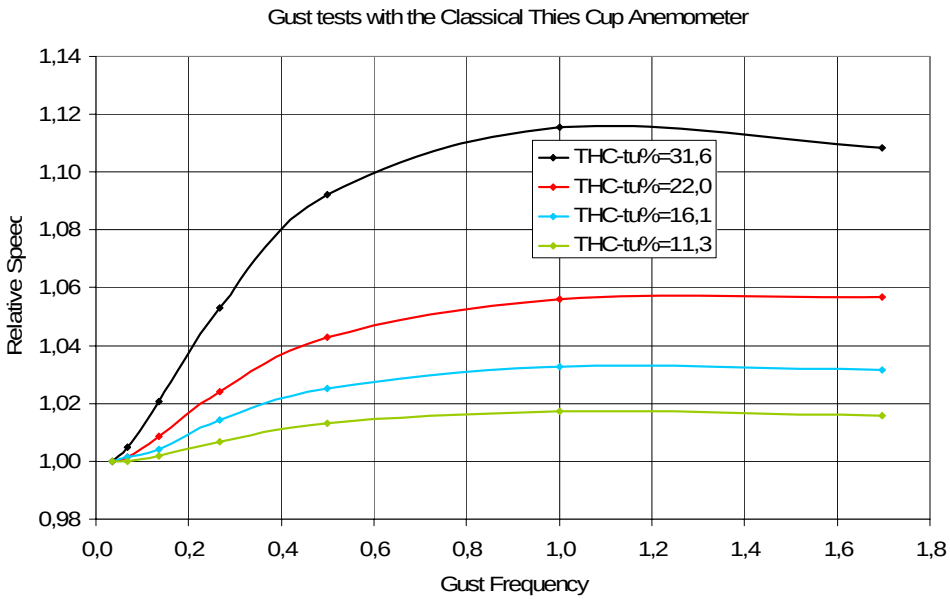

Figure 3-34 Result from gust tests with the classical Thies cup anemometer. The graph shows the ratio between the mean wind speed as seen by the anemometer and the average of the propellers. The highest over-speeding is about 12%.

3.11 Step Response Measurements

A step response test method is described in [15]. It is carried out by exposing the anemometer to constant wind speed (U_{TARGET}) and repeatedly stop and release the rotor and measure the pulse train from the anemometer. This exercise is carried out several times for wind speeds at 5, 8 & 11m/s.

The distance constant (Dist) is determined from the pulse train by fitting an exponential function *U(t)* to the measured data, were *t* is measured from each time of release of the anemometer, see Figure 3-35.

$$U(t) = U_{TARGET}(1 - \exp^{-t/\tau})$$

The distance constant is then given by:

$$Dist = U_{TARGET} \cdot \tau$$

www.PartoSystem.com

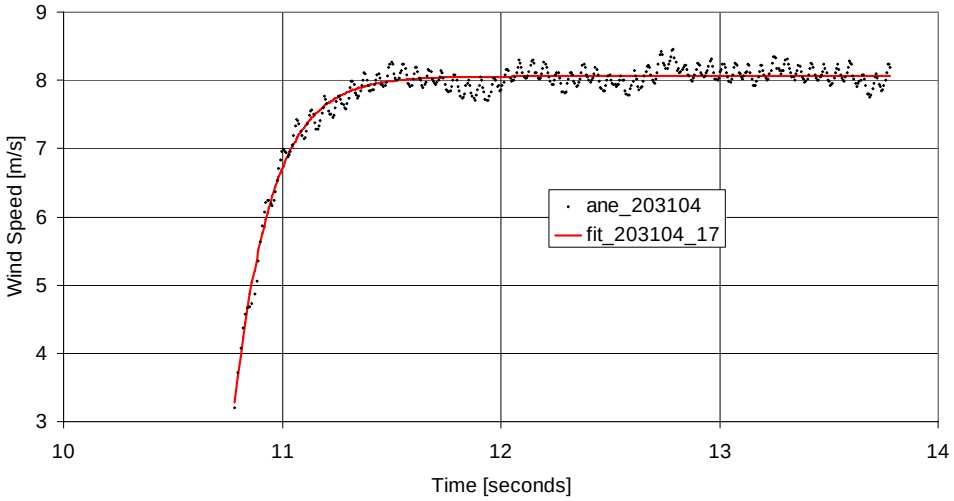

Figure 3-35 The graph shows the response from a typical step response test at 8 m/s wind speed. From the graph each pulse from the anemometer can be seen. The variation in rotational speed due to the three cups is clearly visible. The red curve is fitted to the pulses to establish the time constant and the distance constant.

Table 3-3 shows the determined distance constants from a number of tests. The distance constant varies randomly, due also to the position of release, between 1.1m and 1.6m, with an average of 1.346m and a standard deviation of 0.13m.

Table 3-3 Step response measurements of a cup anemometer

file	step	time	target	dist	fit-error	average	std
050901_202530	1	9,016	5,173	1,199	3,567		
050901_202530	2	13,739	5,135	1,458	2,423		
050901_202530	3	18,621	5,215	1,476	3,099		
050901_202530	4	23,665	5,137	1,209	3,520		
050901_202530	5	29,316	5,148	1,557	4,423		
050901_202530	6	34,722	5,160	1,309	3,056		
050901_202530	7	39,504	5,125	1,417	3,360		
050901_202530	8	45,045	5,170	1,273	2,283		
050901_202530	9	51,344	5,182	1,567	2,985		
050901_202530	10	56,815	5,152	1,282	2,415		
050901_202530	11	63,813	5,228	1,477	2,251		
050901_202530	12	70,166	5,238	1,455	2,998		
050901_202530	13	76,011	5,108	1,323	2,557		
050901_202530	14	81,503	5,084	1,143	2,508		
050901_202530	15	86,910	5,142	1,152	2,967	1,353	0,143
050901_203104	17	10,695	8,060	1,376	9,911		
050901_203104	18	18,041	8,124	1,158	11,839		
050901_203104	19	24,446	8,051	1,238	13,296		
050901_203104	20	31,167	8,111	1,179	10,598		
050901_203104	21	38,957	8,074	1,423	10,140		
050901_203104	22	46,383	8,137	1,323	13,956		
050901_203104	23	53,374	8,067	1,229	11,262		
050901_203104	24	60,832	8,097	1,418	13,636		
050901_203104	25	67,485	8,089	1,368	15,371		
050901_203104	26	75,153	8,114	1,401	13,080		

www.PartoSystem.com

050901_203104	27	83,593	8,088	1,541	10,842		
050901_203104	28	90,339	8,177	1,217	15,974		
050901_203104	29	97,022	8,096	1,453	9,059	1,333	0,118
050901_203327	30	10,784	11,196	1,280	26,436		
050901_203327	35	17,018	11,302	1,216	28,910		
050901_203327	36	23,274	11,322	1,292	31,310		
050901_203327	38	30,501	11,151	1,094	28,683		
050901_203327	39	37,054	11,254	1,421	31,722		
050901_203327	40	43,792	11,230	1,581	34,161		
050901_203327	41	50,475	11,214	1,505	38,492		
050901_203327	42	57,616	11,266	1,451	32,915		
050901_203327	43	63,991	11,188	1,419	28,768		
050901_203327	44	70,209	11,148	1,317	30,331		
050901_203327	45	77,544	11,205	1,305	26,900	1,353	0,139
					all	1,346	0,131

3.12 Bearing Friction Measurements

Bearing friction measurements have been described in [5,14]. Friction in bearings of cup anemometers adds a small negative torque on the rotor which reduces the rotational speed a small amount. The friction depends on the design and lubrication of the bearings. Often friction increases significantly at lower temperatures due to higher viscosity of the lubrication substance. Friction in bearings can be measured with a flywheel test. The rotor of the cup anemometer is dismantled from the shaft, and a flywheel is fitted. The flywheel should have the same weight as the rotor, so that the loading of the bearings can be considered the same. The flywheel should also have a sufficiently high inertia, so that the rotor will keep spinning for a reasonably long time, a minute or more, for the best conditions. It is important that the deceleration is not too fast, since this will reduce the measurement sensitivity.

Friction must be measured under constant temperature conditions. Such conditions can be made in a closed climate chamber, where the rotor is excited by a remote mechanism. An example of such an arrangement is shown in Figure 3-36, where the excitation is applied through a motor, driving a wheel with a rubber ring, and applied to the flywheel by shortly activating an electric magnet.

www.PartoSystem.com

Figure 3-36 Bearing friction measurement setup in climate chamber. At left heater, fan, sensors, excitation mechanism, and the mounting of the cup anemometer with the flywheel is show. At right the flywheel and the driving motor is shown in detail.

The motor is set to rotate the cup anemometer at a rotational speed that corresponds to 20-25m/s. On excitation the motor will accelerate the flywheel to this rotational speed, and on release, the flywheel will decelerate due to friction in bearings and air friction on the flywheel.

The deceleration can be described with the differential equation:

$$I\frac{d\omega}{dt} = -F(\omega) - 0.616\pi\rho R^4(\nu\omega^3)^{1/2}$$

Here $F(\omega)$ is friction in bearings as function of angular speed. The second term on the right hand side is the air friction of the flywheel with the radius R [16]. The term is valid for laminar conditions, which is the case for Reynolds numbers below 300.000. For a flywheel of radius 3cm and rotation at 40rad/s, corresponding to 8m/s, the Reynolds number is 2400. Laminar conditions are therefore assumed for all cases during the tests. Table 3-4 lists air data to be used to derive the flywheel friction. It is seen, that although both the air density and the kinematic viscosity changes significantly with air temperature, the formula constant can in general be set to 0.009kg/m^{2}s$^{1/2}$ for the temperatures between 40°C and -20°C.

Table 3-4 Air data for flywheel friction calculations

Air temperature [°C]	Air density ρ [kg/m^3]	Kinematic viscosity ν [m^2/s]	0.616*π*ρ*ν$^{1/2}$ [kg/m^{2}s$^{1/2}$]
-20	1.39	11.2*10^{-6}	0.009002
-10	1.35	12.0*10^{-6}	0.00905
0	1.29	13.0*10^{-6}	0.009001
10	1.25	13.9*10^{-6}	0.009019
20	1.21	14.9*10^{-6}	0.009039
40	1.12	17.1*10^{-6}	0.008963

www.PartoSystem.com

The differential equation can be reduced to:

$$I\frac{d\omega}{dt} = -F(\omega) - 0.009kg/m^2 s^{1/2} \cdot R^4(\omega^3)^{1/2}$$

Isolating the bearing friction term, one gets:

$$F(\omega) = -I\frac{d\omega}{dt} - 0.009kg/m^2 s^{1/2} \cdot R^4(\omega^3)^{1/2}$$

The friction measurement in the climate chamber gives a deceleration curve of angular speed as function of time. This curve is fitted to a 3rd order polynomial, which can easily be differentiated to a 2nd order polynomial. The data are fitted in the interval 4-16m/s only. The friction within the 4-16m/s wind speed interval is again fitted to a second order polynomial:

$$F(\omega) = f_1 + f_2\omega + f_3\omega^2$$

There may be some torque associated with the sensing of the rotational speed of the cup anemometer, which should be included in the bearing friction measurement. The cup anemometer should therefore be electrically connected for measurements during the tests.

Figure 3-37 shows a typical deceleration run with a cup anemometer with two pulses per rev. Such pulses are seldom opposed exactly by 180º, which is indicated by the spreading of data during the deceleration. Figure 3-38 shows the total friction, the flywheel friction, and the deduced bearing friction. Figure 3-39 and Figure 3-40 show measured decelerations and fitted friction of five successive tests at -18°C. The results show good reproducibility. The cup anemometer was a RISØ P2546 cup anemometer, see [14]. Flywheel characteristics were: weight 51g, radius 0,030m, inertia $2{,}30*10^{-5}$ kgm^2. Figure 3-41 show typical measured friction at temperatures form 40°C to -20°C.

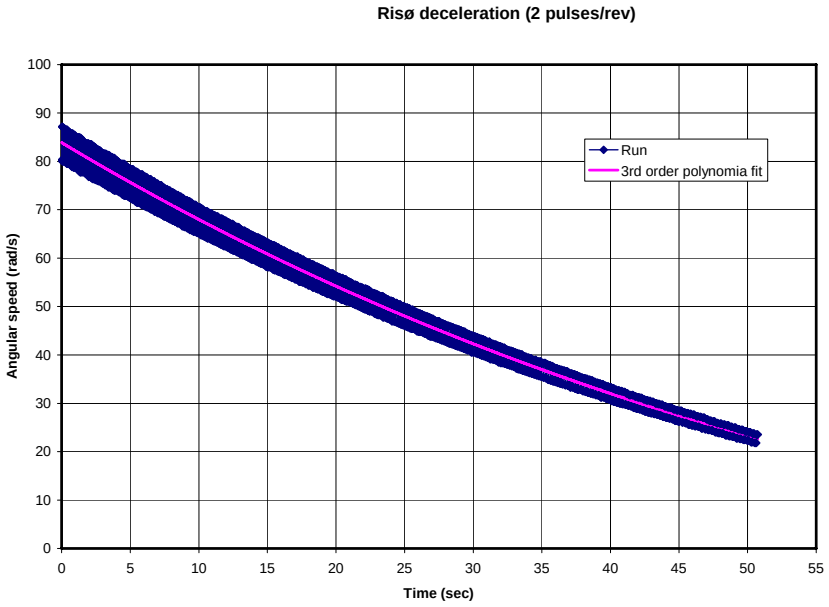

Figure 3-37 Typical deceleration run with a Risø cup anemometer with two pulses per rev at 20ºC

www.PartoSystem.com

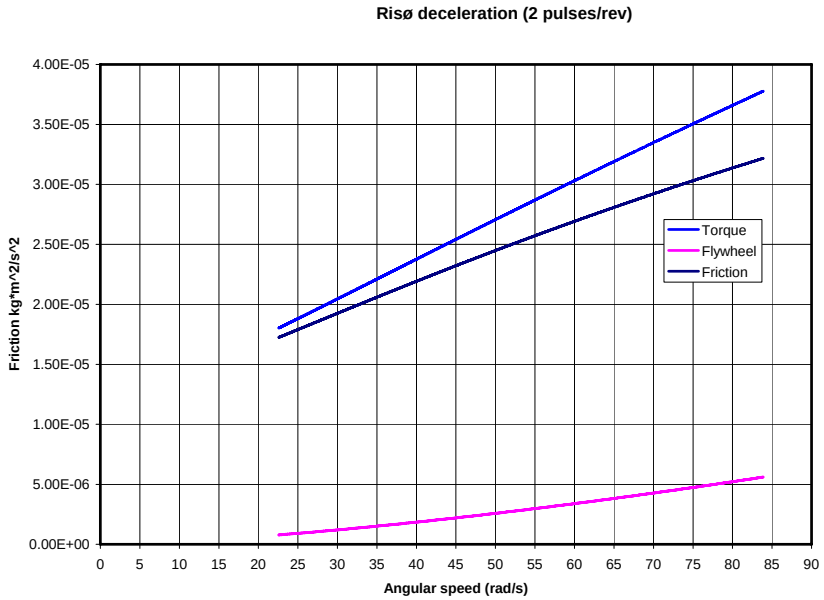

Figure 3-38 Total friction, flywheel friction and bearing friction of Risø cup anemometer as function of angular speed at 20ºC

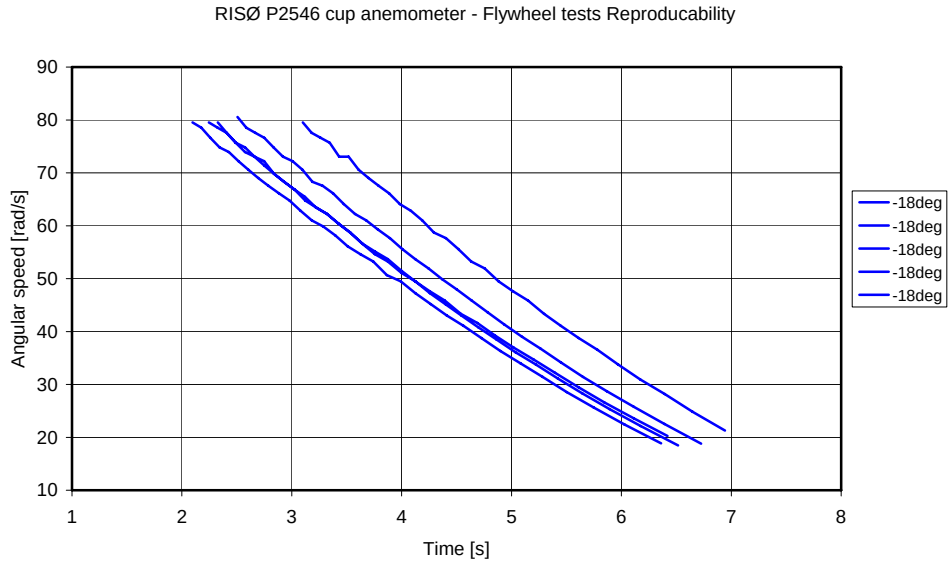

Figure 3-39 Five successive flywheel deceleration tests of RISØ P2546 cup anemometer

www.PartoSystem.com

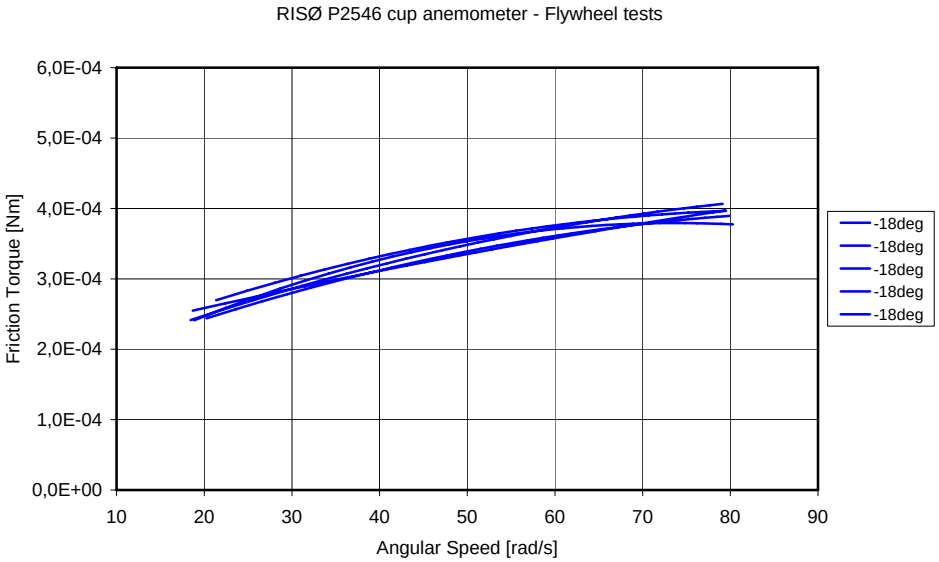

Figure 3-40 Five successive friction torque measurements of Risø cup anemometer

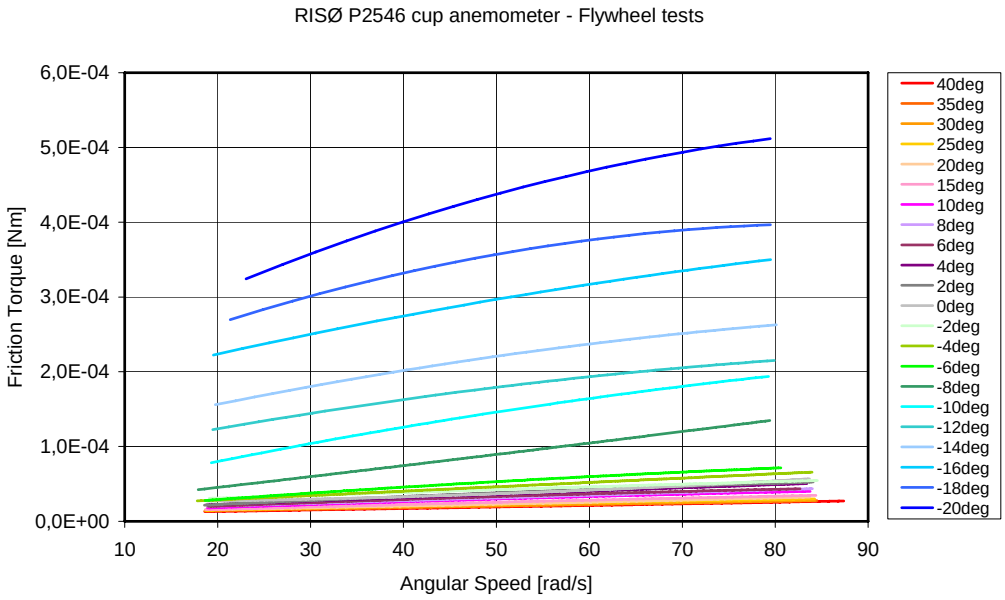

Figure 3-41 Friction measurements of Risø cup anemometer [14]

www.PartoSystem.com

3.13 Rotor Inertia Measurements

The cup anemometer rotor inertia is measured by a simple oscillation method in which the rotor is set to oscillate around its axis, see Figure 3-42.

Figure 3-42 Determination of moment of inertia by oscillations of a Vector cup anemometer rotor. Length of strings 0.8m.

The rotor is set to oscillate with a not too high amplitude as the air damping will influence on the cups. A number of oscillations is made, and the average time of one oscillation determined.

From the oscillation tests, the inertia can be found from the formula:

$$I = \frac{T^2 Mgr^2}{4\pi^2 l}$$

where:

T	is average time of one oscillation
M	is mass of rotor
r	is radius from axis of rotation to the three strings
l	is the length of the strings
g	is gravitational acceleration ~9.81m/s^2

www.PartoSystem.com

4. Time Domain Modelling of Cup-Anemometers

4.1 Introduction

Modelling of cup anemometers is known since 1929, where Schrenk [17] measured torque on cup anemometers to analyse dynamic characteristics. Several scientists have since then made modelling of cup anemometers, and improvements have been made with better insight in the physics of the instruments. Two time domain models are presented in the following chapters. The use of the models in simulation for classification of five cup anemometers is presented in report [8].

The first model was developed in the CLASSCUP project [5]. It is in this report referenced as the Tilt-Response&Torque-Coefficient model (TRTC). It is based on a measured tilt response, a measured torque coefficient curve for horizontal flow, and measured bearing friction curves. This model is also described in annex J of the IEC standard [7].

The second model, here referenced as the Inclined-Flow-Torque-Coefficient model (IFTC), is based on measured torque coefficient curves for a range of inclined flow angles. This new model is developed in the ACCUWIND project, and is only available due to the possibility to measure torque coefficient curves under inclined flow conditions.

The cup anemometer rotor torque is in both models calculated from instantaneous 3D wind time traces, derived by artificial wind generators representing turbulent field wind conditions, see chapter 5.

4.2 Generalization of the rotor torque

Normalization of the rotor torque was originally proposed by Schrenk [17]. He normalized measured torque to parabolas. Normalization of rotor torque to one torque coefficient curve was also demonstrated in the CLASSCUP project [5]. The torque on one cup of a RISØ cup anemometer was measured in the FFA LT5 wind tunnel for varying angular speed and varying wind speed. The torque measurements are shown in Figure 4-1 and Figure 4-2.

www.PartoSystem.com

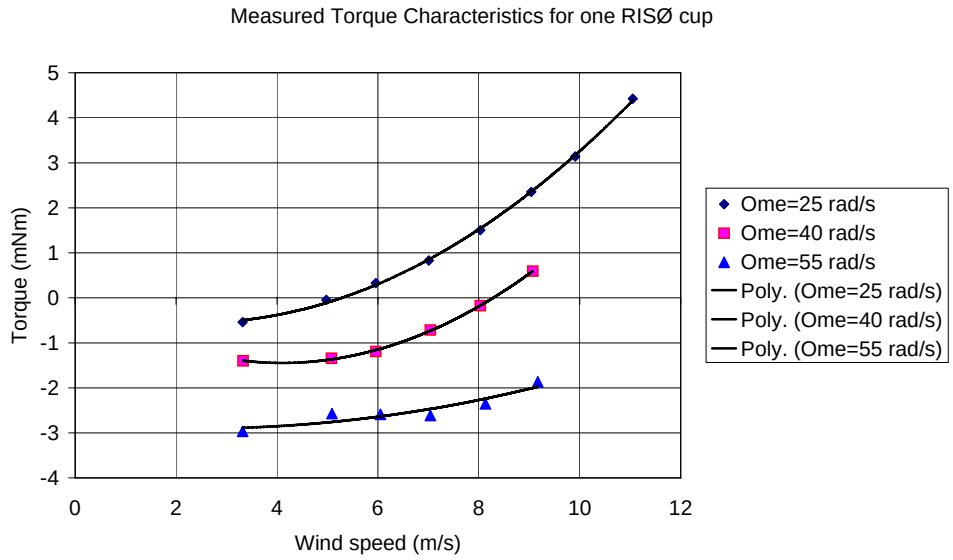

Figure 4-1 Measured torque curves for RISØ cup anemometer (one cup) with fixed rotational speed and varying wind tunnel speeds

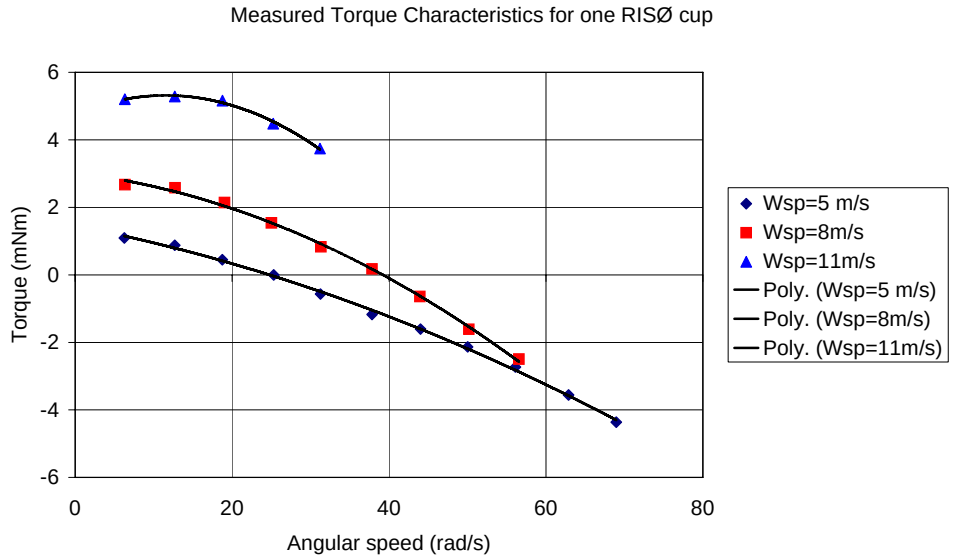

Figure 4-2 Measured torque curves for RISØ cup anemometer (one cup) with fixed wind tunnel speed and varying rotational speeds

The measured torque curves of Figure 4-1 and Figure 4-2 can be generalized nicely to one normalized torque coefficient curve, where the torque coefficient is defined as:

$$C_{QA} = \frac{Q_A}{\frac{1}{2}\rho A R U^2}$$

Q_A is rotor torque, i.e. in this example three times one cup torque. The measured torque should be subtracted bearing friction torque before normalization in clearing that the torque coefficient represents pure rotor aerodynamics.

www.PartoSystem.com

The speed ratio, being the x-axis in the normalized torque coefficient curve, is defined by:

$$\lambda = \frac{\omega R}{U - U_t}$$

The wind speed U is subtracted a threshold wind speed U_t which corresponds to most of the offset in the calibration line. The rest and small part of the offset is due to friction. The introduction of a threshold wind speed is a necessity that makes the measured and normalized torque coefficient curve consistent with the static calibration expression at zero torque. In the case of no friction the speed ratio can be transformed into a calibration expression:

$$\lambda = \frac{\omega R}{U - U_t} \Leftrightarrow U = \frac{\omega R}{\lambda} + U_t \Leftrightarrow \omega = \frac{\lambda}{R}(U - U_t)$$

All measured data from Figure 4-1 and Figure 4-2 are normalized and shown in Figure 4-3. The figure shows that all data collapse into one curve. The measured data are seen to fit reasonably well to a parabola. It should be mentioned though, that parabolas do not describe the important details of the torque curve, which are necessary for realistic simulation of cup anemometer dynamics.

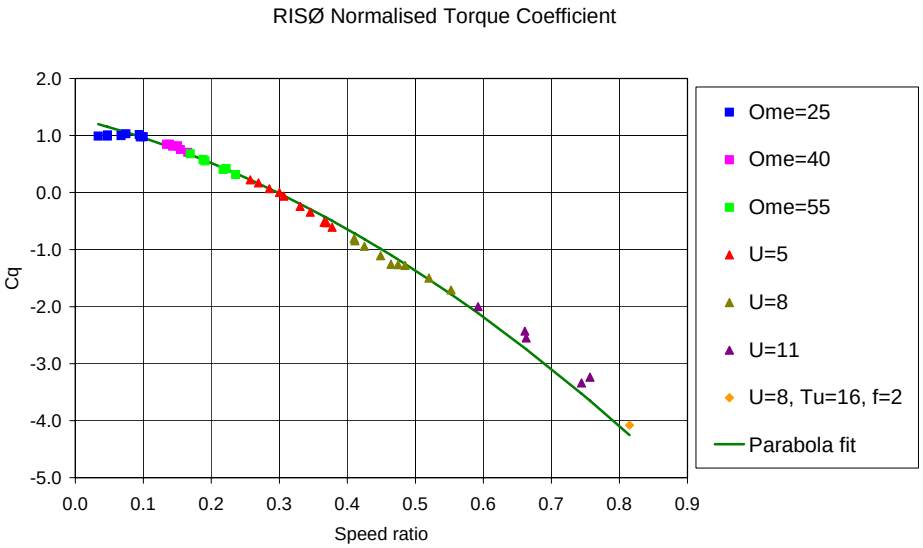

Figure 4-3 Normalized torque coefficient of the RISØ cup anemometer for various wind speeds and angular speeds

4.3 The Tilt-Response & Torque-Coefficient Model (TRTC)

The TRTC model assumes the forces on the cup anemometer rotor to be based on a torque, due to aerodynamic forces on the rotor and a friction torque in bearings, due to lubrication and contact of moving surfaces. The aerodynamic torque is dependent on wind speed, angular speed of the rotor and flow inclination angle, and the friction torque is dependent on temperature and angular speed of the rotor, so the total torque can be expressed as:

$$Q = Q_A(U, \omega, \alpha) - Q_F(T, \omega)$$

Q_A is the aerodynamic torque on the rotor and Q_F is the friction torque in bearings, a positive quantity. The aerodynamic torque is expressed in terms of

www.PartoSystem.com

the angular response curve and the normalized torque coefficient curve for horizontal flow conditions, which are combined to give the total aerodynamic torque.

Angular response

The instantaneous wind vector is reduced to an equivalent horizontal wind speed, which is assumed to generate the same aerodynamic torque. First, the instantaneous wind vector for the time t is determined from the artificial wind generator:

$$\vec{U} = (u, v, w)$$

Where u, v, w are the longitudinal, the transversal and the vertical wind speed components respectively. The instantaneous flow inclination angle is:

$$\alpha = A\tan\frac{w}{\sqrt{u^2 + v^2}}$$

The influence of the flow inclination angle is expressed in the angular response curve of the cup-anemometer, and is dependent on flow inclination angle and wind speed, in this case the scalar of the wind vector is substituted with the constant wind tunnel wind speed:

$$U_{vec} = \left|\vec{U}\right| = \sqrt{u^2 + v^2 + w^2}$$

The equivalent horizontal flow wind speed U_{eq} is derived from the scalar wind vector by multiplication with the angular response $F_\alpha(U_{vec}, \alpha)$:

$$U_{eq} = F_\alpha(U_{vec}, \alpha) \cdot U_{vec}$$

The angular response is linearly interpolated between, at first wind speed curves, then flow angle.

Aerodynamic torque for horizontal flow

For the horizontal flow conditions with the equivalent horizontal flow wind speed, the aerodynamic torque is derived from the torque coefficient curve. First, the speed ratio is determined:

$$\lambda = \frac{\omega R}{U_{eq} - U_t}$$

The torque coefficient curve $C_{QA}(\lambda)$ can either be fitted to a higher order polynomial, forced through the equilibrium speed ratio (speed ratio at zero torque) with a higher order (for instance 11) or be tabulated. The aerodynamic torque is determined by:

$$Q_A = \frac{1}{2}\rho A R U^2 C_{QA}(\lambda)$$

Bearing friction

Bearing friction is linearly interpolated between parabolic friction curves at different temperatures:

$$Q_F = f_0(T) + f_1(T) \cdot \omega + f_2(T) \cdot \omega^2$$

Where f_0, f_1, f_2 are constants for given temperatures.

Total driving torque

The driving torque exerts acceleration on the rotor according to the differential equation:

www.PartoSystem.com

$$I\frac{d\omega}{dt} = Q = Q_A - Q_F$$

In numerical calculations, the acceleration is assumed constant in a short time step t, and a new angular speed is calculated with the Euler method:

$$\Delta\omega = \frac{Q}{I}\Delta t$$

When the angular speed is known, the indicated (measured) wind speed of the cup anemometer is found by applying the calibration expression:

$$U = A_{cal}\omega + B_{cal}$$

This wind speed can then be compared to the "true" wind speed, which in the IEC standard, ref. 8, is defined as the horizontal wind speed:

$$U_{hor} = \sqrt{u^2 + v^2}$$

Deviations, calculated for classification purposes are based on simulation of measurement, often using 10min averaging:

$$U_{dev} = \sum_{10\,\mathrm{min}} U - \sum_{10\,\mathrm{min}} U_{hor}$$

Calculations, based on the TRTC model are shown in [5,8,14].

Fitting of data to the cup anemometer model

In practice, not all characteristics on a cup anemometer can be made under the same conditions. The use of different testing institutes, different wind tunnels, and the variation of atmospheric conditions as temperature and humidity may influence on the measurement results, so a fitting of the data to the model is necessary, for instance as shown in [14, chapter 4.2]. The calibration curve, preferably based on an accredited calibration certificate, is the basis for the fitting process. The process is accomplished by the following steps:

1. Normal calibration in wind tunnel at certain calibration temperature to generate calibration curve
2. Measure angular response curves in wind tunnel
3. Measure torque curves in wind tunnel at certain temperature
4. Measurement of bearing friction in climate chamber
5. Determine bearing friction at temperature for torque curve measurements
6. Add bearing friction to measured torque curves
7. Determine aerodynamic torque coefficient curve
8. Fit aerodynamic torque coefficient curve to linear calibration curve by numerical simulation of calibration so that threshold wind speed and a torque correction value is found

The last point is very important. It is absolutely essential that simulation with the cup anemometer model of the linear calibration is made and fitted successfully if the simulations shall be used for classification purposes. Successfully in this context means that the simulations shall almost not deviate from the calibration line and at least all deviations shall be much less than the individual variations of the calibration points from the line.

www.PartoSystem.com

4.4 The Inclined-Flow-Torque-Coefficient Model (IFTC)

The IFTC model is in many aspects similar to the TRTC model, but deviates in the way aerodynamic torque is simulated. The aerodynamic torque is, as for the TRTC model, dependent on the wind speed, angular speed of the rotor and flow inclination angle, but the IFTC model uses a more direct approach. Once the normalised torque coefficient curves are known for horizontal flow as well as for inclined flow they can be used to find the response of the anemometer when it is exposed to artificial wind conditions including wind variations in all directions. The flow inclination angle is used directly to determine the torque coefficient, and no angular response curve is used.

The simulation procedure in using the IFTC model here is as follows:
Assume friction is insignificant and that the anemometer rotates with an angular speed ω and that wind data (artificial or real) including all three velocity components are known with a high time resolution. (usually 20 Hz or more), then for each time step:

1. Determine the scalar wind speed and inflow angle
2. Determine the speed ratio and the torque coefficient $C_Q(\lambda,\alpha)$ from the database
3. Calculate the torque value
4. Calculate the angular acceleration (deceleration)
5. Calculate the angular speed ω in the next time step
6. Calculate the wind speed indicated by the anemometer

The inflow angle

The scalar vector wind speed is calculated as the resultant of the three wind velocity components:

$$U_{vec} = \sqrt{u^2 + v^2 + w^2}$$

The inflow angle is calculated as the angle between the vertical and the horizontal components.

$$\alpha = A\tan\frac{w}{\sqrt{u^2 + v^2}}$$

Aerodynamic torque at inclined flow

The speed ratio is calculated as:

$$\lambda = \frac{\omega R}{U_{vec} - U_t}$$

The torque coefficient for the present time step is interpolated from the database of torque coefficient curves $C_Q(\lambda,\alpha)$, shown in Figure 3-30. Linear interpolation is used to establish a $C_Q(\alpha)$ table for the present speed ratio. The C_Q value for the present inflow angle is derived from the table by cubic spline interpolation.

The driving torque can now be calculated according to:

$$Q = \frac{1}{2}\rho A R U_{vec}^2 C_q$$

www.PartoSystem.com

Determination of measured wind speed
The angular acceleration is calculated according to:

$$\frac{d\omega}{dt} = \dot{\omega} = \frac{Q}{I}$$

This acceleration is assumed to be constant and so the angular speed at the next time step is given by:

$$\omega_{t+\Delta t} = \omega_t + \dot{\omega} \cdot \Delta t$$

When the rotational speed of the anemometer is known, the wind speed indicated by the anemometer is calculated using the standard calibration constants.

The use of the IFTC model on five cup anemometers is shown in [8].

5. External Conditions for Cup Anemometer Classification

5.1 External Operational Conditions

The conditions for classification of cup anemometers in this report refer to the classification system presented in the IEC standard, ref. 8. The standard has two classification categories for cup anemometers. The first, category A, relates to "ideal" sites, which consist of reasonably flat terrain, where the terrain influence is small on power curve measurements. The second, category B, relates to complex sites that do not meet the requirements of an "ideal" or reasonably flat site, and where the terrain influences significantly on power curve measurements.

Table 5-1 show the operational ranges required for the classification categories in the IEC standard. The table includes information on the wind spectra being used in this report with 350m longitudinal length scale for the Kaimal spectrum for Class A, and 170m length scale for the isotropic von Karman spectrum for Class B.

Table 5-1 Operational ranges of Class A and Class B category classification

www.PartoSystem.com

	Class A Terrain meets requirements in annex B of standard		Class B Terrain does not meet requirements in annex B of standard	
	Min	Max	Min	Max
Wind speed range to cover [m/s]	4	16	4	16
Turbulence intensity	0,03	0,12+0,48/V	0,03	0,12+0,96/V
Turbulence structure $\sigma_u/\sigma_v/\sigma_w$	1/0,8/0,5 (non-isotropic turbulence) Kaimal wind spectrum with a longitudinal turbulence length scale of 350m		1/1/1 (isotropic turbulence) Von Karman wind spectrum with a longitudinal turbulence length scale of 170m	
Air temp. [°C]	0	40	-10	40
Air density [kg/m^3]	0,9	1,35	0,9	1,35
Average flow inclination angle [°]	-3	3	-15	15

5.2 Wind speed range

Most wind speed measurements in wind energy applications are related to wind resource and wind utilisation purposes. For these purposes 10 minute averages are used. The IEC standard [7], and Table 5-1 requires the 10 minute average wind speed range 4-16m/s for classification purposes. Below 4 m/s the power in the wind is insignificant and above 16 m/s, the power from the wind turbine is regulated to be almost constant and independent of the wind speed, so the 4-16m/s range is appropriate for this analysis.

5.3 Turbulence ranges

5.3.1 Turbulence intensity levels

The IEC safety standard [18], gave guidance as to the relevant range of turbulence intensities for design of wind turbines. The IEC standard on performance measurements [7], uses similar expressions for the turbulence ranges. The maximum standard deviations of the wind speed for Class A requirements are:

$$\sigma_1 = 0.48m/s + 0,12V_{hub} \Rightarrow Ti = \frac{0.48m/s}{V_{hub}} + 0,12$$

The equivalent requirements for class B are:

$$\sigma_1 = 0.96m/s + 0,12V_{hub} \Rightarrow Ti = \frac{0,96m/s}{V_{hub}} + 0,12$$

The maximum turbulence for class A requirements are thus 24% at 4m/s and 15% at 16m/s, and for class B 36% at 4m/s and 18% at 16m/s, respectively. The lowest turbulence intensities that are considered in the IEC standard [7] are 3% at all wind speeds. Figure 5-1 shows the turbulence intensity ranges for class A and class B requirements.

www.PartoSystem.com

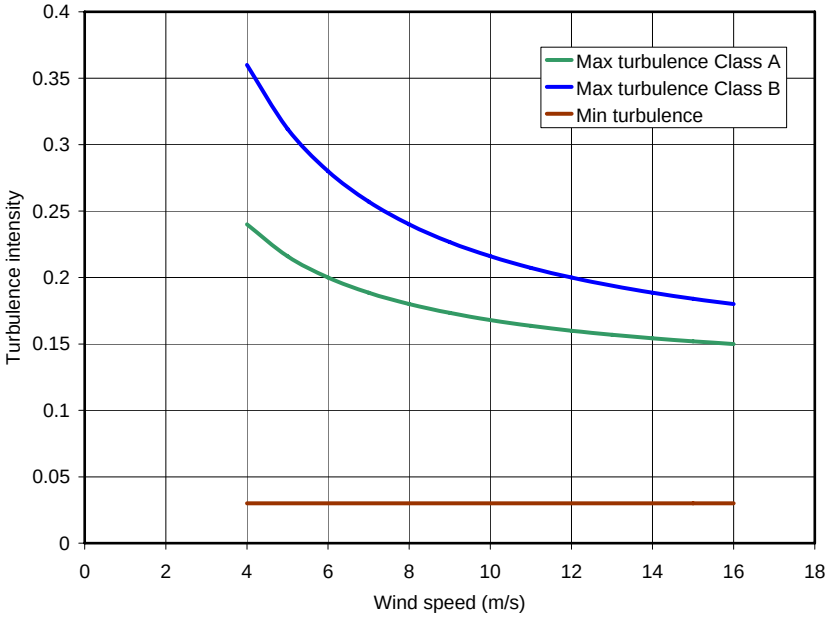

Figure 5-1 Turbulence intensity ranges as function of wind speed for class A and class B requirements

5.3.2 Turbulence spectra

The three-dimensional turbulent wind spectra are site specific, and do seldom follow the general average spectra, but for classification purposes it is appropriate to apply standard spectra. The spectra being applied in this IEC safety standard [18] are the Kaimal spectrum model for non-isotropic conditions and the von Karman spectrum model for isotropic conditions. These spectra are also applied here.

The Kaimal spectra of the three turbulence components, used for class A cup classification, are modelled by:

$$\frac{fS_k(f)}{\sigma_k^2} = \frac{4fL_k/U}{(1+6fL_k/U)^{5/3}}$$

The average wind speed U, the standard deviations σ_k and the length scales L_k, where the k index indicate the longitudinal, transversal and vertical turbulence components are parameters for which their ranges must be determined. The relation between the standard deviations and the length scales in the spectra are shown in Table 5-2.

Table 5-2 Standard deviations and length scales for the three turbulence component Kaimal spectra

	Longitudinal	Transversal	Vertical
Standard deviation σ_k	σ_1	$0.8\cdot\sigma_1$	$0.5\cdot\sigma_1$
Integral length scale L_k	L_1	$0.33\cdot L_1$	$0.08\cdot L_1$

In the IEC safety standard [18], the longitudinal length scale L_1 for heights above 30m is determined as 170m, while it is required to be set equal to 350m in the IEC power performance measurement standard [7]. This is a factor 2,3 times higher.

www.PartoSystem.com

The average length scale of the longitudinal spectrum is varying over a broad spectrum. For a specific site at Vindeby [19], the longitudinal length scales have been analysed for both onshore (LM) and offshore positions (SMS and SMW), as shown in Figure 5-2. The dashed curves are for 3m height.

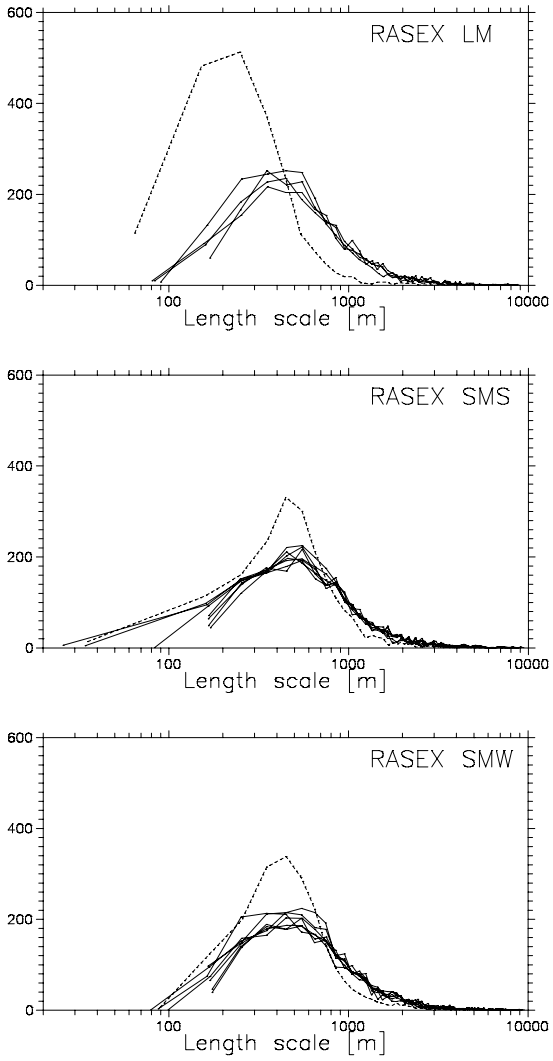

Figure 5-2 Longitudinal length scales measured onshore and offshore at Vindeby [19].

The longitudinal length scale of 350m shows good agreement with the requirement measured average length scales in Figure 5-2.

In the IEC power performance standard [7] it is required to use the Kaimal spectrum. For clarity, the Kaimal spectrum is defined for non-isotropic turbulence while the von Karman is defined for isotropic turbulence conditions. The von Karman is for this work used for Class B classification with a length scale of 170m, as shown in Table 5-1. This length scale is equivalent to the 350m length scale of the Kaimal spectrum.

www.PartoSystem.com

The von Karman isotropic turbulence spectrum, used for class B cup classification in this study, being the same for all three turbulence components, is modelled by:

$$\frac{fS_k(f)}{\sigma_k^2} = \frac{4fL_k/U}{(1+71(fL_k/U)^2)^{5/6}}$$

In the IEC safety standard [18], the longitudinal length scale L_1 for a von Karman spectrum for heights above 30m is determined to be 74m. Using the same relative length scale factor of 2.3 for the Kaimal spectrum, as found for the von Karman spectrum, the length scale is set to 170m.

5.4 Air temperature ranges

The environmental air temperature is the temperature to which the cup-anemometer is exposed, but not necessarily the temperature of the bearings, which might be heated in several types of cup-anemometers. The air temperature ranges of operational wind turbines are according to the IEC safety code [18] -10°C to 40°C for normal conditions and -20°C to 50°C for extreme conditions. The temperature range -10°C to 40°C corresponds to the requirements of Class B classification in Table 5-2. Though the table include temperatures down to -10°C the category does not specifically consider conditions with rime, snow and ice, and such conditions are not taken into account in the present analysis. The Class A category is avoiding rime, snow and icing conditions as the temperature range is limited to 0°C to 40°C.

5.5 Air density range

The air density range is in Table 5-2 required to vary between 0.90 to 1.35 kg/m^3. The air density is affecting the ratio of frictional forces to aerodynamic forces on cup anemometers. This ratio becomes significant when temperatures are low and lubricants increase viscosity or when cup anemometers have small cups and rotor arms compared to size of bearings. For altitudes from sea level up to 2000m the standard air density ranges from 1.225 to 1.006 kg/m^3, according to ISO Standard Atmosphere [20]. For a constant altitude a typical air density range of ±10%, including air humidity variations, is normal. The air density range for a power performance measurement is thus adequate for the classification.

5.6 Flow inclination angle ranges

During power performance measurements the flow inclination varies. For a flat test site (Risø test site, Roskilde, Denmark) the flow inclination varies during a measurement period as shown in Figure 5-3.

www.PartoSystem.com

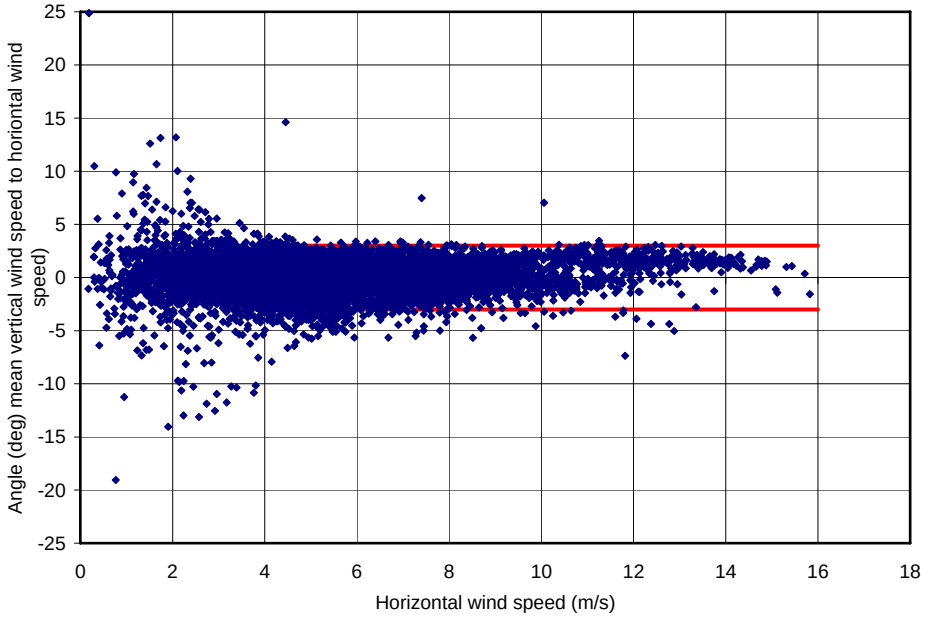

Figure 5-3 Variations of flow inclination angle (mean vertical component to mean horizontal component) for a flat site at 30m height (Risø, Roskilde, Denmark)

Figure 5-3 shows that measured flow inclination angles vary a little more than the required range in Table 5-1 at low wind speeds for a Class A cup classification. Wind turbine sites and power performance measurements are performed also in mountainous terrain where the slope of the terrain may be high. To cover such applications, a range of flow inclination angles of -15° to 15° for class B in Table 5-1 seems reasonable, as the terrain slopes themselves may be of this size.

5.7 Artificial 3D Wind Generators

In modelling cup anemometers it is important to know in detail the wind input. It is thus very appropriate to use artificial 3D wind generators to generate wind with the required characteristics as required in Table 5-1 for.

Several artificial wind generators are available. The wind generators used for the present analysis are made by Jakob Mann [21]. They are made of two algorithms, one called Kaimal.exe, the other vonKarman.exe, generating wind from the Kaimal and von Karman models, respectively.

The algorithms simulate turbulent atmospheric wind fields, and are based on a model of the spectral tensor for atmospheric surface-layer turbulence at high wind speeds They simulate three-dimensional fields of three components of the wind velocity fluctuations. The spectral tensor has been compared with and adjusted to several spectral models used in wind engineering, for example the Sandia method [22].

www.PartoSystem.com

6. Application of Classification Procedures

6.1 Classification of cup anemometers

The calibration methods, the two cup anemometer models, TRTC and IFTC, and the external operational conditions according to the IEC performance measurement standard [7], and Table 5-1 have been applied to five different types of cup anemometers for classification. The results are presented in the report ref. 8. Results of the IFTC model are shown without influence of friction, and results of the TRTC model are shown for angular response measurements made by both DEWI and FOI.

6.2 Robustness of applied procedures

There are many steps in making a classification of a cup anemometer. First of all, the calibrations: normal calibration, angular response calibration, torque calibration and friction calibration have uncertainties. The calibrations deviate in different methods being used, and in different institutes applying the procedures. As an example, variations in Round Robin tests of normal calibrations between cup anemometer calibration institutes within the MEASNET organization are of the order of 1%.

Cup anemometer models vary. They vary with the parameters they take into account and how they interpolate data, and they vary how well they simulate the physical characteristics.

Robustness of classification procedures is reached when the application of the procedures gives almost the same results for different institutes performing the classification and for different approaches with sufficient capability being applied. This chapter will deal with some aspects of robustness of the procedures being applied.

6.3 Calibration Robustness

6.3.1 Differences in normal calibrations

In the MEASNET organization web site [23] regular Round Robin tests are performed in order to keep track of the deviations between the cup anemometer calibration institutes. The organization has rules that require all calibration institutes to perform calibrations within 1% of average. This requires the calibration procedure in the IEC power performance measurement standard [7] being applied. In 1985 when a common cup anemometer calibration procedure was unavailable, a Round Robin test varied between calibration institutes by 6%.

www.PartoSystem.com

6.3.2 Differences in tilt response measurements

Measurements of static angular response of a range of cup anemometers have been carried out by FOI and DEWI in the ACCUWIND project. The deviation between these measurements can be regarded as a measure of the robustness of one quantity used in the classification process namely the angular response. The deviations between FOI and DEWI for the five examined anemometers are presented in Figure 6-1 to Figure 6-6.

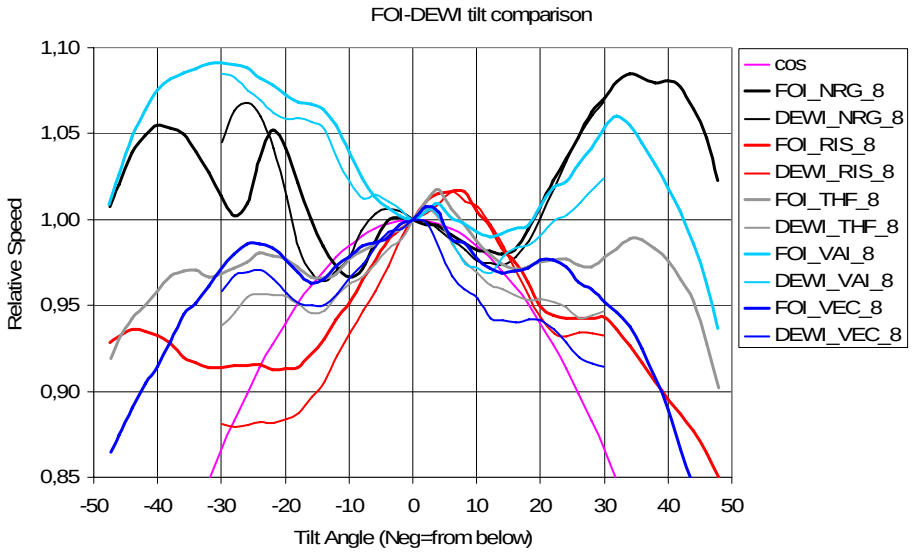

Figure 6-1 Angular response measurements on five cup anemometers by FOI and DEWI at 8m/s

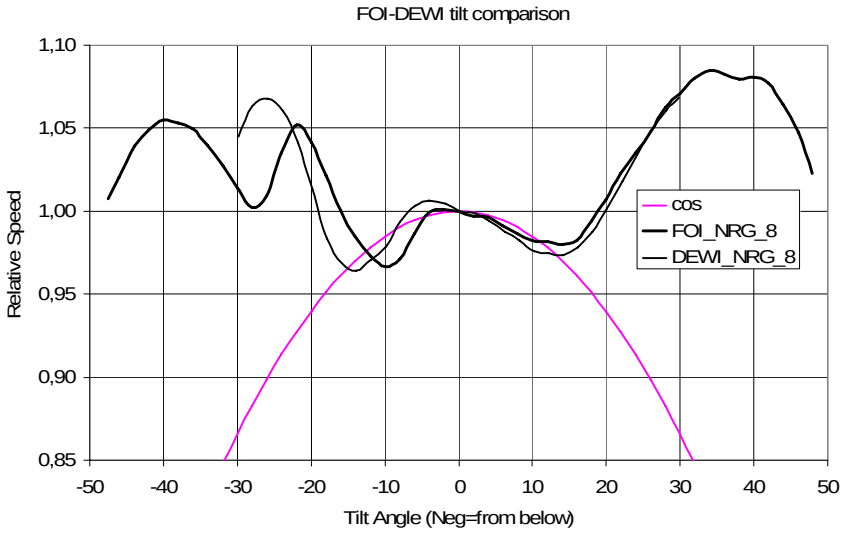

Figure 6-2 Angular response measurements on NRG cup anemometer by FOI and DEWI at 8m/s

www.PartoSystem.com

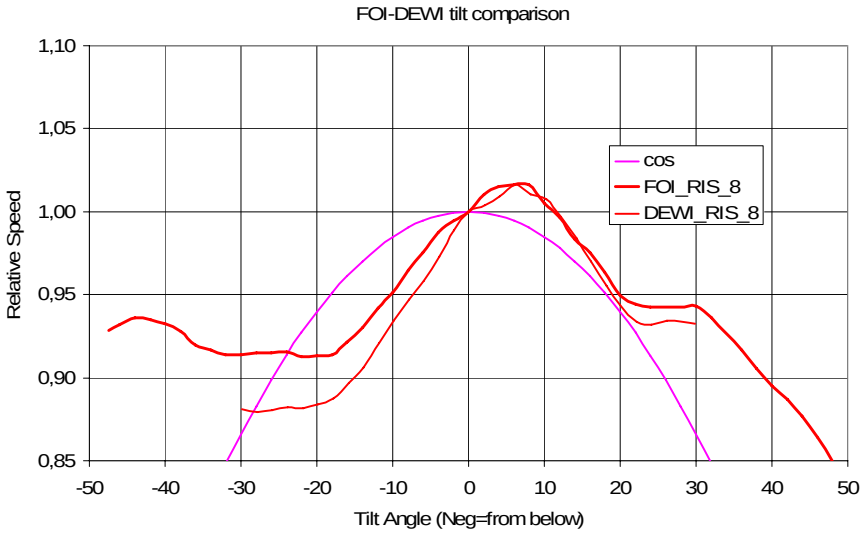

Figure 6-3 Angular response measurements on Risø cup anemometer by FOI and DEWI at 8m/s

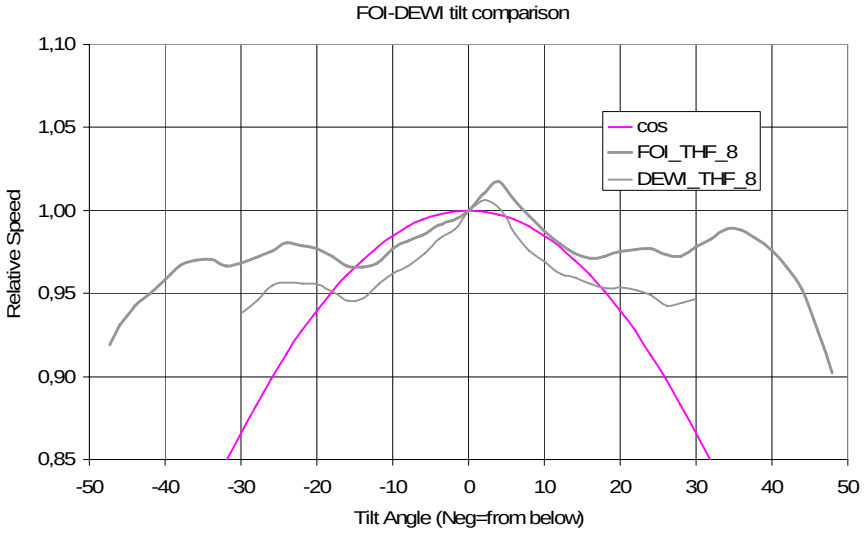

Figure 6-4 Angular response measurements on Thies First Class cup anemometer by FOI and DEWI at 8m/s

www.PartoSystem.com

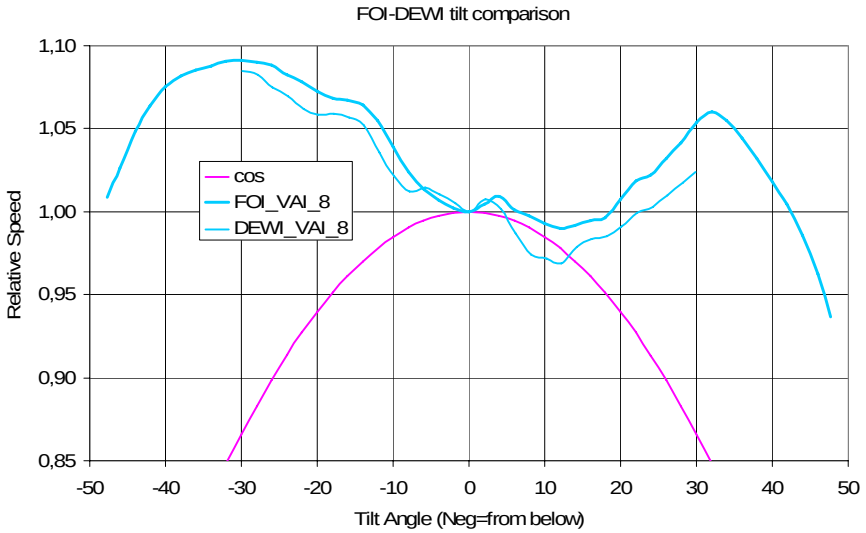

Figure 6-5 Angular response measurements on Vaisala cup anemometer by FOI and DEWI at 8m/s

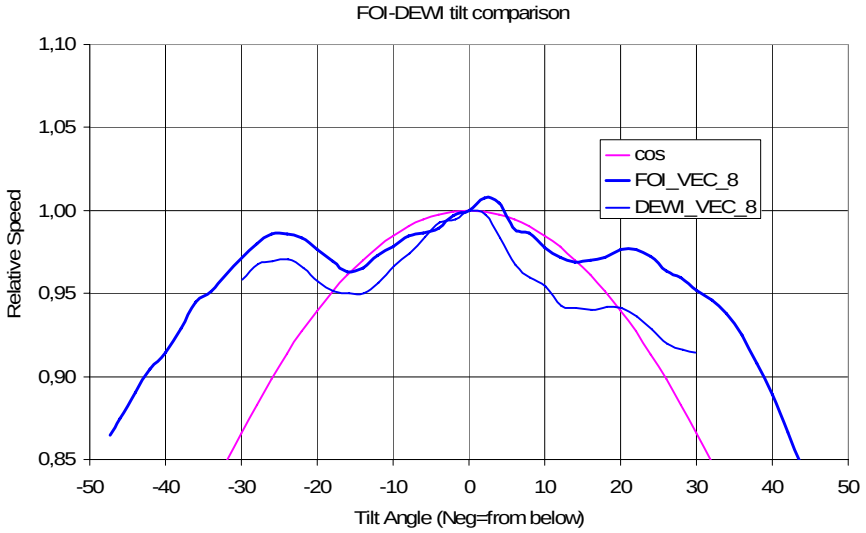

Figure 6-6 Angular response measurements on Vector cup anemometer by FOI and DEWI at 8m/s

The causes for the deviations in the calibrations have not been examined in detail. FOI is using a closed test section and the anemometer is moved back and forth in the test section to obtain different tilted positions. The wind tunnel used by DEWI is an open test section and the anemometer rotor centre is kept fixed for all tilted positions.

6.3.3 Differences due to inertia

As demonstrated in section 3.7.3 it was necessary to adjust the torque coefficient values used in the in-direct torque measurement method for both the Risø and the Thies classical cup anemometers to match the direct measured normalized torque curves. The Cq values for the Risø anemometer were scaled up by

www.PartoSystem.com

7% and the Cq values for the Thies anemometer were scaled up by 6%. One of the scale factors used in the formula to derive the torque curves is the cup inertia. In section 3.7.4 it was discussed if the differences could be caused by too low cup inertia.

To demonstrate how an error in any of the scale factors influence the calculation of the class-index a sensitivity calculation was performed. The inertia values of the five commercial cup-anemometers were changed ±20% from the nominal values. This gave rise to a maximum change in the class-index of less than 1% for all anemometers.

This shows that the accuracy of the absolute values of the scale parameters are of lesser importance. A scale up of Cq corresponds to an increased torque available for acceleration of the rotation but also an increased (negative) torque available for deceleration of the rotation. It is the details around the equilibrium, i.e. the balance between the two sides that counts.

6.4 Cup Anemometer Model Robustness

The most robust model of a cup anemometer is capable to simulate any controlled flow condition, especially all calibration flow conditions, where the calibration results are fitted to the model.

6.4.1 Simulation of normal calibration

The most important simulation, as mentioned in Chapter 4.3, is a simulation of a normal calibration. A normal calibration is the best controlled flow condition a cup anemometer can be exposed to. The model must be able to simulate the calibration line very accurately, see Figure 6-7, where the TRTC model simulates a calibration line [14]. For cup anemometers quite sensitive to friction, this calibration line will vary with temperature.

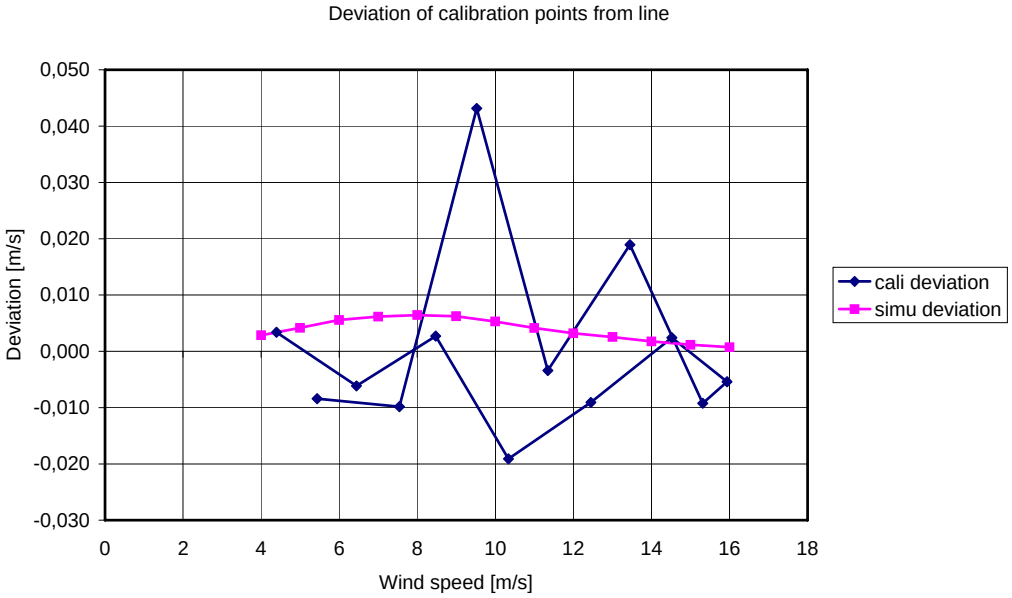

Figure 6-7 Deviations from calibration line for a calibration and a corresponding simulation of a Risø cup anemometer [14]

www.PartoSystem.com

6.4.2 Comparison of measured and calculated step response

Another well-controlled flow condition is a step response measurement; see Figure 6-8, where the step response results from the measurements presented in Chapter 3.11. The step response is compared with a corresponding calculated step response by a simulation with the IFTC model. Figure 6-8 shows a quite good fit of measured and calculated data. The measurement of a step response is difficult, though, when number of pulses per rev is small.

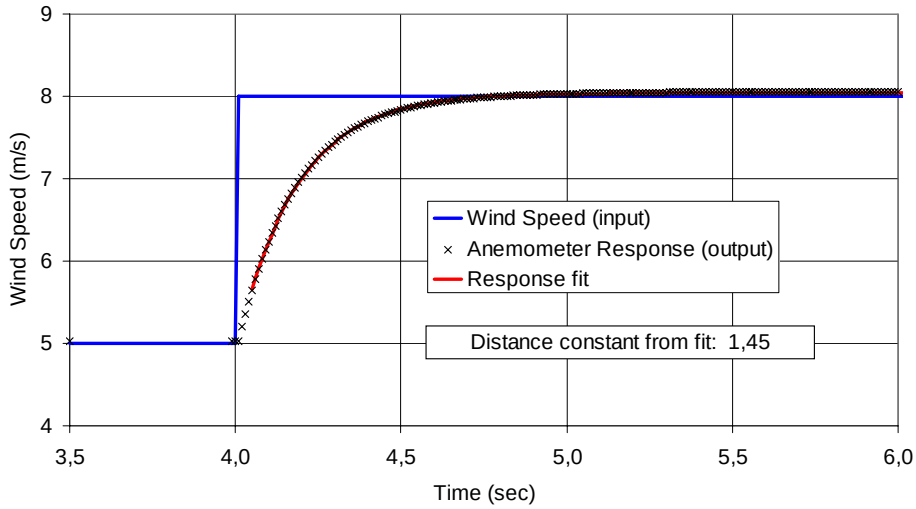

Figure 6-8 Calculated step response for an anemometer based on measured $C_Q(\lambda)$ *and applied step change. The distance constant from the calculation and fitted value 1.45 agrees rather well with the measured values 1.35±0.13 of Chapter 3.11.*

6.4.3 Comparison of measured and calculated response from gust runs

Gust run measurements with pure horizontal flow presented in Chapter 3.10, and demonstrated in Figure 3-32 to Figure 3-34, also represent reasonably well controlled flow conditions. The dynamic response expressed as overspeeding can be compared with corresponding calculated values using the IFTC model. This comparison should give an indication on how well the procedure works under pure horizontal conditions.

As input to the calculations the derived torque database $C_Q(\lambda,\alpha)$ and pure sinusoidal wind sequences were used. The wind sequences were generated with wind variations only in the longitudinal component and amplitudes and gust frequencies similar to the gust measurements (as seen by the propellers). Figure 6-9 shows a comparison for the classical Thies anemometer.

www.PartoSystem.com

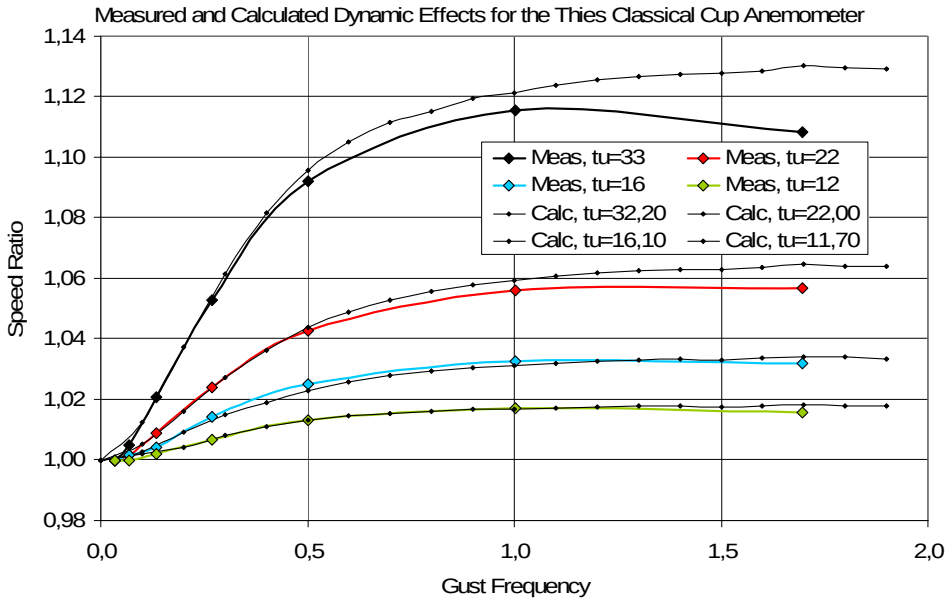

Figure 6-9 Comparison of measured and calculated response from gust tests with the classical Thies cup anemometer.

The agreement in Figure 6-9 is very good at lower gust frequencies. The deviations at higher gust frequencies are caused by the fact that the tunnel can not maintain the high amplitudes. The wind speed as indicated by the propellers show a reduction in turbulence (amplitudes) at the highest frequency by approximately 3-8%. A more thorough comparison would be to use the actual wind speed sequences from the propellers in the calculations instead of the generated constant amplitude sequences.

6.5 Robustness of Classification

Classification is robust when calibration procedures are robust, cup anemometer models are robust, and when classification results are almost the same when performed by different institutes on different examples of the same cup anemometer make and type. In this respect it must be mentioned that one type of cup anemometer varies in calibration line in normal calibrations and over time, and this is the reason why cup anemometers are calibrated separately, and before and after a power curve measurement. A spreading of classification results should therefore also be expected.

A comparison of four classifications is made on a Risø type cup anemometer, according to the IEC power performance standard [7], and Table 5-2. Classification 1 in Table 6-1 is made with the TRTC model [14], based on tilt and torque measurements by FOI, normal calibration by DEWI, and friction and inertia measurements by Risø. The external operational conditions in Table 5-1 were different from [7], so a re-calculation was made. Classifications 2, 3 and 4 in Table 6-1 are based on another cup anemometer of the same type. Classification 2 is also made with the TRTC model. Normal calibration, tilt and torque measurements are made by FOI, and friction and inertia measurements are made by Risø. Classification 3 is the same as 2, except that the tilt response measurement is made by DEWI, Figure 6-3. Classification 4 is made with the IFTC model. Normal calibration, inclined flow torque coefficients and inertia are de-

www.PartoSystem.com

termined from inclined flow measurements by FOI. The results of the four classifications are shown in Table 6-1.

Table 6-1 Four classifications of Risø cup anemometer with variations in angular response

Classification no	Class A Category Horizontal	Class B Category Horizontal	Class A Category Vector	Class B Category Vector
1) TRTC, R-1364 report	1.3	6.1	1.8	10.2
2) TRTC, FOI tilt response	1.4	5.1	1.7	9.2
3) TRTC, DEWI tilt response	1.9	8.0	2.4	12.0
4) IFTC no friction	1.3	5.0	1.7	9.2

The four classifications in Table 6-1 show reasonably good correlations, but also with a specific deviation that need a comment. Classification 3 deviates from the others in significantly higher class values for all categories. The reason for this should be found in the angular response differences in Figure 6-3. The DEWI angular response curve is for negative tilt angles significantly lower than the FOI curve even for small tilt angles.

Another comparison of classifications is made focusing on the influence of friction. In this case classifications were made on a cup anemometer that has relatively high friction torque compared to aerodynamic torque. Classifications 5 and 6 in Table 6-2 correspond to the conditions of classification 2 in Table 6-1, with and without friction. Classifications 7 and 8 correspond to the conditions of classification 3, respectively, and conditions of 9 correspond to 4. All classifications are shown in Table 6-2.

Table 6-2 Five classifications of NRG cup anemometer with variations in friction

Classification no	Class A Category Horizontal	Class B Category Horizontal	Class A Category Vector	Class B Category Vector
5) TRTC, FOI tilt, with friction	2.4	8.3	2.7	3.0
6) TRTC, FOI tilt, no friction	1.0	8.3	0.8	2.2
7) TRTC, DEWI tilt, with friction	2.4	7.7	2.8	4.8
8) TRTC, DEWI tilt, no friction	1.9	7.7	2.1	4.4
9) IFTC no friction	0.6	7.5	0.5	2.6

The classifications in Table 6-2 show significant variations, especially for the Class A categories, with or without friction. The deviations were analysed with a parameter analysis. For a 4m/s, 3% turbulent wind, and for temperatures 0°C, 40°C and 18°C (the calibration temperature), the density was varied 0.9-1.35kg/m^3. The results are shown in Figure 6-10.

www.PartoSystem.com

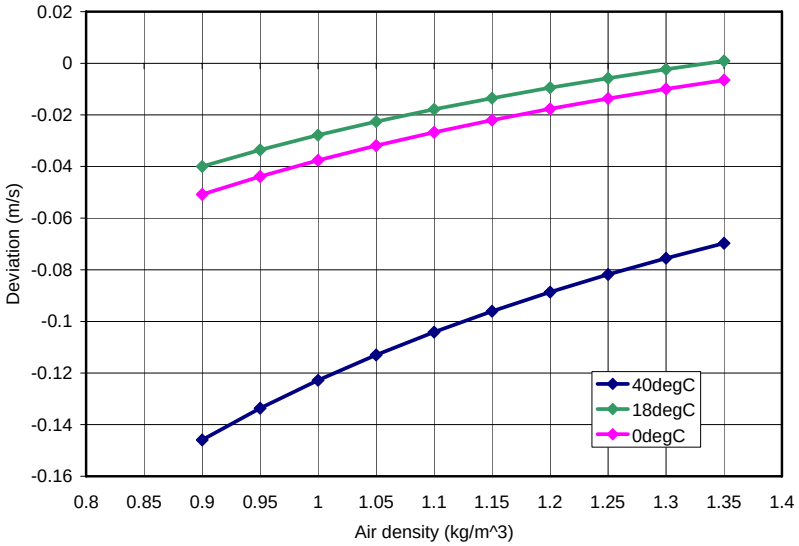

Figure 6-10 Simulated deviations due to variations in temperature and air density of NRG cup anemometer at 4m/s and 3% turbulence

The deviations in Figure 6-10 show a high dependence on temperature. Measured friction on the NRG cup anemometer is shown in Figure 6-11. The measured friction at 40°C does deviate from friction at the lower temperatures, and this seems to explain the significant variations of Table 6-2. In looking at five friction runs that were actually made in the tests, Figure 6-12, it is seen that there is a very high spreading in the data. Whether this is caused by the cup anemometer or spreading due to the test method is at present not investigated. Running the classification calculations with a maximum temperature of 30°C with the FOI tilt angular response gives the classification indices in Table 6-3. The results are seen to lower the Class A horizontal classification index from 2.4 in Table 6-2 down to 1.1.

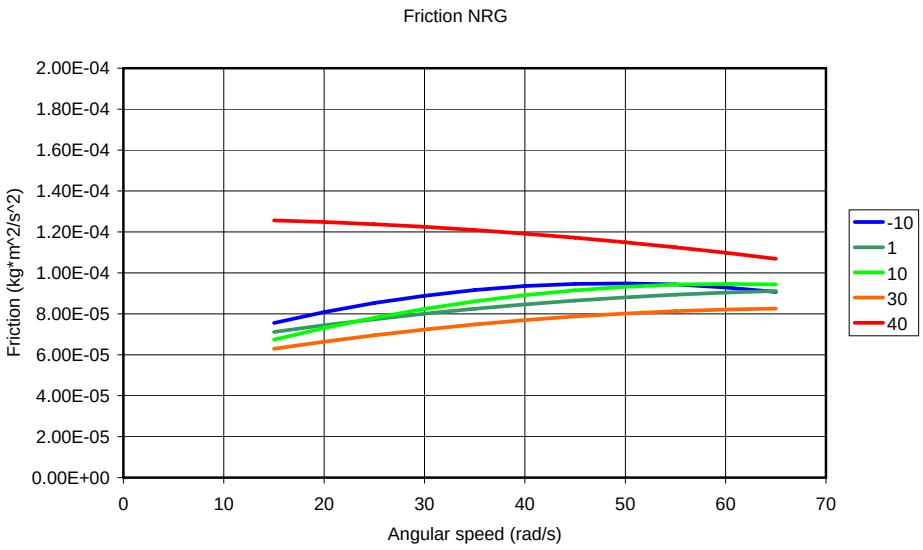

Figure 6-11 Measured friction on NRG cup anemometer

www.PartoSystem.com

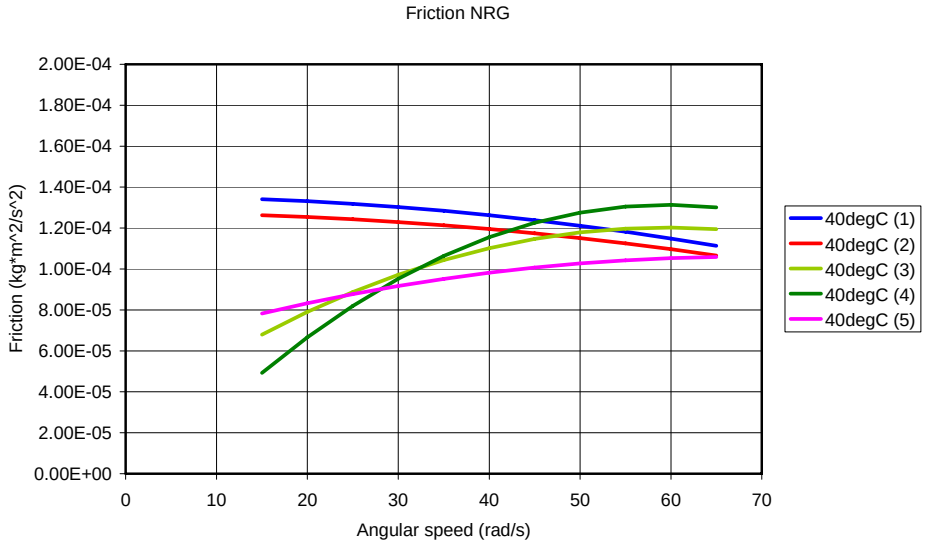

Figure 6-12 Five measurements of friction on NRG cup anemometer at 40°C

Table 6-3 Classification of NRG cup anemometer with variations in friction up to maximum 30°C

Classification no	Class A Category Horizontal	Class B Category Horizontal	Class A Category Vector	Class B Category Vector
10) TRTC, FOI tilt, with friction To max 30degC	1.1	8.3	1.2	3.0

These classification examples show that the classification index may change significantly by changes in measurements and modeling. In this respect it should be noted that there do not exist standards or recommendations of the measurement procedures of angular response, torque coefficients and friction in the same way as for normal calibrations. More common use of these measurement procedures, Round Robin exercises between testing institutes, and more common use of the cup anemometer models may reduce the classification index variations. On the other hand, the examples demonstrate that the classification process is very efficient in detecting which characteristics has the most influence on the class index of individual cup anemometer. One general weak characteristic of most cup anemometers is the rather high gradients on angular response around horizontal flow. Small changes in the angular response do immediately influence the Class A index. Some cup anemometer designs also very efficiently demonstrate insensitivity to friction. The classification tools do in this way also demonstrate very efficiently their capability to improve on cup anemometer design.

6.6 Free Field Comparison Tests

6.6.1 Free Field Tests Compared to Simulations

The ultimate verification of the IFTC model capability to predict the cup anemometer behaviour would be to compare detailed field measurements with calculated anemometer response. This requires that the 3D wind field is accurately

www.PartoSystem.com

known in detail both at the cup anemometer position and at the reference position. Such measurements have not been possible to perform in this project. The only available simultaneous measurements with cup anemometer and 3D sonic data have been taken from the comparable measurements of two sonics, ref. 26. mounted on a boom together with a Risø anemometer. From these measurements the cup/sonic response ratio has been derived by binning the ratio as function of turbulence intensity.

Neither the details of the spectral content from the boom measurements nor the turbulence components have been evaluated. Instead it is assumed that the turbulence components correspond to a flat site with ratios 1/0.8/0.5 between the u, v and w turbulence components. In order to enable a comparison the measured cup/sonic response ratio also had to be adjusted such that this ratio was approaching unity when going from higher to lower turbulence intensities. The graph below shows the "comparison".

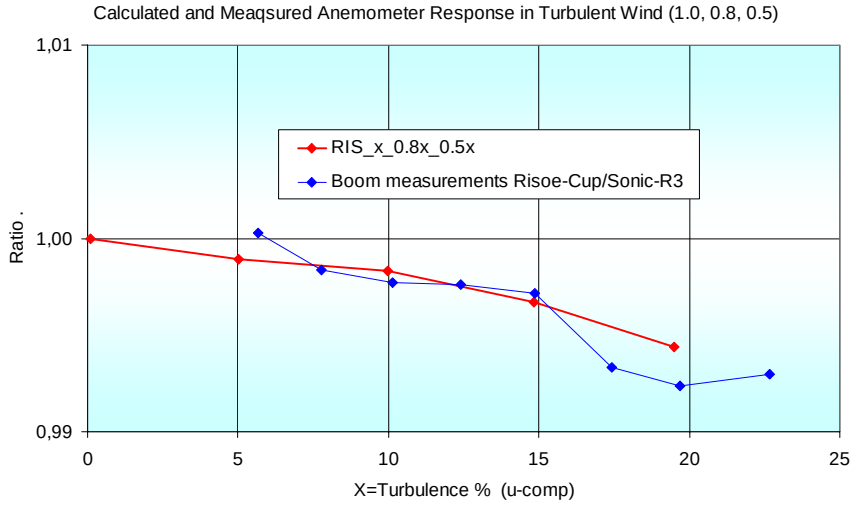

Figure 6-13 "Comparison" of measured and calculated response to turbulence for the Risø anemometer.

6.6.2 Influence of Free Field Horizontal Shear Flow

All models do make assumptions that in the end limit their usefulness. The models described in the earlier chapters are limited in their description of the flow field that drives the aerodynamic torque of the cup anemometers. The calibrations, statically as well as dynamically, are assuming uniform flow across the area of the cup anemometers. The flow in the models is also considered uniform when an external artificial wind field is applied on the anemometers, and it is considered a point measurement, representing the centre of the instrument. In the free field the flow is not uniform. The flow consists of shears and vortices in all directions, and these influence on the aerodynamic torque of the cup anemometers. A shear that is applied horizontally across the frontal area of a cup anemometer is specifically influential to the cup anemometer as the shear applies different resulting forces on either side of the cup anemometer. A study of such shear flow was made by Dahlberg [24] where the shear effect around masts was studied. The effect was studied in theory applying a drag model of

www.PartoSystem.com

the cup anemometer. A shear flow with a relative wind speed difference ε at the centre of the advancing cup and $-\varepsilon$ at the centre of the retrogressive cup is applied in the model:

$$Q_A = R(D_H - D_L) = \frac{1}{2}\rho AR((U(1-\varepsilon) - R\omega)^2 C_{DH} - (U(1+\varepsilon) + R\omega)^2 C_{DL})$$

Rearranging the terms, it is seen that the relative wind speed difference can be considered as an addition to the speed ratio:

$$Q_A = R(D_H - D_L) = \frac{1}{2}\rho ARU^2((1-(\lambda+\varepsilon))^2 C_{DH} - (1+(\lambda+\varepsilon))^2 C_{DL})$$

This means that the speed ratio changes with the relative wind speed difference ε, and the equilibrium speed ratio changes for a constant wind as:

$$\lambda_0 = \frac{1-\sqrt{k}}{1+\sqrt{k}} - \varepsilon$$

The angular speed of the cup anemometer will thus change to:

$$\omega = \frac{U}{R}(\lambda_0 + \varepsilon)$$

The change in angular speed corresponds also to a change in an equivalent planar wind speed:

$$U = \frac{\omega R}{\lambda_0 + \varepsilon}$$

This shear effect leads to small variations in the measurements in a mast whether a cup anemometer is positioned on the one or the other side of the mast when the boom is perpendicular to the wind. A positive shear on one side will give a little higher value, while a negative shear on the other side will give a little lower value. This effect is opposed when the rotational direction of the cup anemometer is changed.

An experiment was made in a wind tunnel [25] where an ordinary fine fishing net with a mesh width of 8.5mm and a thread thickness of 0.15 mm was inserted in half the test section. A cup anemometer was then traversed behind the net and the wind speed of the cup anemometer was measured. The measurements showed a 1,5% lower wind speed when the cup anemometer was fully behind the net relative to free flow, but when partially behind the net a difference of about 2.5% to 2.9% was found. For a typical speed ratio λ_0 of 0.3 and an ε value of 0.75%, the difference is calculated to be 2.5%. This corresponds quite well with the measurements in the wind tunnel.

7. Conclusions

The present report addresses cup anemometer classification methods, based on the requirements in the IEC61400-12-1 standard on power performance measurements [7]. An introduction of the ideas behind the classification procedure is outlined in chapter 2, and the requirements for external operational conditions are examined in detail in chapter 5. Chapter 3 presents a range of different testing methods that all support robust assessment of the cup anemometers. Some basic testing methods are used to provide data to be fitted to cup anemometer models, the IFTC and the TRTC models (Chapter 4), and other testing methods are used for verification of the tuned models to “check” that they are able to

www.PartoSystem.com

simulate operational conditions realistically. The basic testing methods are: normal calibration, angular response measurements, static torque coefficient measurements, and measurement of friction.

An additional new dynamic torque coefficient test method was developed. It involves exposure of the anemometers to wind gusts in a wind tunnel together with accurate measurements of the instantaneous wind speed and of the rotational speed of the cup-anemometer. The method requires no attachment of a rod to the rotor as for the static torque coefficient measurement. This new method was compared to the more traditional static torque coefficient measurement procedure, and very good agreement was found between the two methods. The new dynamic torque coefficient test method has the advantage that torque can be measured under inclined flow by tilting the cup anemometer in the wind tunnel. This has given rise to the new cup anemometer model, the IFTC model, which bases the aerodynamic torque on dynamic torque coefficient measurements alone, and do not include angular response measurements in the model.

The robustness of the IFTC model was verified by comparing simulations with ordinary gust runs in the wind tunnel, and very good agreement was found. Simulations were also compared with step response measurements with good result. The inclined flow torque coefficient curves of the IFTC model was used to compare static angular response measurements. This comparison showed no deviations between the data. This verifies that angular response data obtained by static measurements are similar to data obtained by dynamic measurements.

The application of the procedures has been examined in Chapter 6. The robustness of the classification process depends on robustness of the calibration procedures, robustness of the models, and general robustness of application. The calibration of angular response was compared with measurements of FOI and DEWI. Significant differences were found in the measured data. The causes for the deviations in the calibrations have not been examined in detail. FOI is using a closed test section and the anemometer is moved back and forth in the test section to obtain different tilted positions. The wind tunnel used by DEWI is an open test section and the anemometer rotor centre is kept fixed for all tilted positions. The differences influence significantly on the results of classification, and are the main reason for spreading of classification index data.

The robustness of the models was demonstrated with the IFTC model by verification of simulations to a step response and to response from gust runs. An example of verification of the TRTC model was made for a normal calibration.

The robustness of classification was exemplified by a comparison of four classifications made with both the TRTC and IFTC models on one type of cup anemometer. The results showed variations of Class A index of 1.3-1.9 and of Class B index of 5.0-8.0. The main reason for these deviations was found in angular response differences measured at DEWI and FOI.

Another classification example of five simulations on another cup anemometer type was made with inclusion and exclusion of friction. The result showed variations of Class A index of 0.6-2.4 and of Class B index of 7.5-8.3. The large variations in Class A index was found to be due to measured friction variations at 40°C. Reduction of the temperature variation to 30°C reduced the Class A index from 2.4 to 1.1.

www.PartoSystem.com

The two cup anemometer models were used to make classification of five different cup anemometers. The results are presented in a separate report [8].
The results of this classification according to the horizontal wind speed definition were:

- NRG in Class A 0.6-2.4, in Class B 7.5-8.3
- Risø in Class A 1.3-1.9, in Class B 5.0-8.0
- Thies FC in Class A 1.5-1.8, in Class B 2.9-3.8
- Vaisala in Class A 1.6-2.4, in Class B 11.0-11.9
- Vector in Class A 1.3-1.8, in Class B 4.0-4.5

The classification of the five cup anemometers shows some variation. The variations have more or less been explained by the exemplifications made for assessment of robustness. The results are based on single examples of the type of cup anemometer. The IEC61400-12-1 standard requires at least two examples of a type of cup anemometer to be tested.

www.PartoSystem.com

8. References

[1] A.Albers, SiteParIden; Relatieve Power Curve Measurements in Flat Terrain, Final report of Task 6, report JOR3-CT98-0257-DEWI07, 13 June 2001-12-07

[2] A.P.W.M. Curvers and P.A. van der Werff, , SiteParIden; Relative Power Curve Measurements in Complex Terrain, Final report of Task 7, report ECN-C—01-102, October 2001.

[3] Albers, A., Klug, H., Westermann, D. ”Outdoor Comparison of Cup Anemometers”, DEWEK 2000

[4] Albers, A., Klug, H., ”Open Field Cup Anemometry”, EWEC 2000

[5] Dahlberg, J.-Å., Gustavsson, J., Ronsten, G., Pedersen, T.F., Paulsen, U.S., Westermann, D., “Development of a Standardised Cup Anemometer suited to Wind Energy Applications”, Contract JOR3-CT98-0263, Publishable Final Report; June 2001

[6] Dahlberg, J.-Å., Pedersen, T.F., Westermann, D., “Development of a Standardised Cup Anemometer suited to Wind Energy Applications, CLASSCUP”, EWEC 2000

[7] IEC 61400-12-1, first edition 2005-12, Wind turbines – Part 12-1: “Power performance measurements of electricity producing wind turbines”

[8] Dahlberg, J-Å, Pedersen, TF, “ACCUWIND – Classification of Five Cup Anemometers According to IEC61400-12-1”, Risø-R-1556(EN), May 2006

[9] IEC 60688: 1992, Electrical measuring transducers for converting a.c. electrical quantities to analogue or digital signals, Amendment 1 (1997), Amendment 2 (2001)

[10] IEC 60044-1:1996, Instrument transformers - Part 1: Current transformers, Amendment 1 (2000)

[11] IEC 60044-2:1997, Instrument transformers - Part 2: Inductive voltage transformers, Amendment 1 (2000)

[12] Pedersen, T.F. “Development of a Classification System for Cup Anemometers – CLASSCUP”, Risø-R-1348(EN), December 2002

[13] Pedersen, T.F. “On Wind Turbine Power Performance Measurements at Inclined Airflow”, Wind Energy, 2004; 7:163-176

[14] Pedersen, T.F. “Characterisation and Classification of RISØ P2546 Cup Anemometer”, Risø-R-1364 (ed.2) (EN), March 2004

[15] IEA Recommended practices for wind turbine testing and evaluation. 3. Fatigue Loads, edition 1990

[16] Schlichting “Aerodynamic Drag”, page

[17] Schrenck O. “Über die Trägheitsfehler des Schalenkreuz-Anemometers bei schwankender Windstärke”, Zeitschrift f. techn. Physik, 1929

[18] IEC 61400-1, second edition 1999 “Wind turbine generator systems – Part 1: Safety requirements”

[19] Frandsen S., Chacón L., Crespo A., Enevoldsen P., Gómez-Elvira R., Hernández J., Højstrup J., Manuel F., Thomsen K. “Measurements on and modelling of offshore wind farms”, Risø-R-903(EN, 1996

[20] ISO 2533 “Standard Atmosphere” 1975

www.PartoSystem.com

[21] Mann J “Wind field simulation”, Probabilistic Engineering Mechanics 13(4): 269-282, Oct 1998
[22] Veers, P. S., Three-dimensional wind simulation. Technical Report SAND88-0152, Sandia National Laboratories, 1988
[23] www.measnet.org
[24] Dahlberg, J-Å, Mast, Boom & Velocity Gradient Effects on Cup Anemometers, FFAP-V-009
[25] Ronsten, G, Dahlberg, J-Å, Calibration of Anemometers in FFA-L2 Wind Tunnel Including Twin Calibration and Tests of Sensitivity to Wind Velocity Gradient and Tilt, FFA TN 1996-51
[26] Cuerva A, Sanz-Andrés A, Franchini S, Eecen P, Busche P, Pedersen TF, Mouzakis F, ACCUWIND, Task 2. Improve the Accuracy of Sonic Anemometers, final report, May 2006

www.PartoSystem.com

Author: Jan-Åke Dahlberg (FOI), Troels Friis Pedersen (Risø), Peter Busche (DEWI)
Title: ACCUWIND - Methods for Classification of Cup Anemometers
Department: Wind Energy Department

Risø-R-1555(EN)
May 2006

Abstract (max. 2000 char.):

Errors associated with the measurement of wind speed are the major sources of uncertainties in power performance testing of wind turbines. Field comparisons of well-calibrated anemometers show significant and not acceptable difference. The European CLASSCUP project posed the objectives to quantify the errors associated with the use of cup anemometers, and to develop a classification system for quantification of systematic errors of cup anemometers. This classification system has now been implemented in the IEC 61400-12-1 standard on power performance measurements in annex I and J. The classification of cup anemometers requires general external climatic operational ranges to be applied for the analysis of systematic errors. A Class A category classification is connected to reasonably flat sites, and another Class B category is connected to complex terrain, General classification indices are the result of assessment of systematic deviations. The present report focuses on methods that can be applied for assessment of such systematic deviations. A new alternative method for torque coefficient measurements at inclined flow have been developed, which have then been applied and compared to the existing methods developed in the CLASSCUP project and earlier. A number of approaches including the use of two cup anemometer models, two methods of torque coefficient measurement, two angular response measurements, and inclusion and exclusion of influence of friction have been implemented in the classification process in order to assess the robustness of methods. The results of the analysis are presented as classification indices, which are compared and discussed.

ISSN 0106-2840
ISBN 87-550-3514-0

Contract no.:

Group's own reg. no.:

Sponsorship:

Cover :

Pages: 68
Tables: 9
References: 26

Risø National Laboratory
Information Service Department
P.O.Box 49
DK-4000 Roskilde
Denmark
Telephone +45 46774004
bibl@risoe.dk
Fax +45 46774013
www.risoe.dk

www.PartoSystem.com

Risø’s research is aimed at solving concrete problems in the society.

Research targets are set through continuous dialogue with business, the political system and researchers.

The effects of our research are sustainable energy supply and new technology for the health sector.

www.PartoSystem.com